

DTIC FILE COPY



Westinghouse

4

REPORT WESTINGHOUSE-O/NPT-723-HYDRO-CR-88-01

AD-A200 896

METAL TRANSFER IN GAS METAL ARC WELDING

Donald M. McEligot and James S. Uhlman, Jr.
Hydrothermodynamics Research and Technology
Westinghouse Electric Corporation
Oceanic Division - Cleveland Operation
(formerly Gould/Ocean Systems Division)
One Corporate Place
Middletown, Rhode Island 02840

DTIC
SELECTED
OCT 13 1988
S D

17 March 1988

Final Report for Period 18 September 1987 to 17 March 1988
Contract Number N00014-87-C-0668

APPROVED FOR PUBLIC RELEASE
DISTRIBUTION IS UNLIMITED

Prepared for
MATERIALS SCIENCE PROGRAM
OFFICE OF NAVAL RESEARCH
800 North Quincy Street
Arlington, Virginia 22217-5000

88 1012 060

UNCLASSIFIED

SECURITY CLASSIFICATION OF THIS PAGE

ADA 200896

REPORT DOCUMENTATION PAGE

1a REPORT SECURITY CLASSIFICATION Unclassified			1b RESTRICTIVE MARKINGS			
2a SECURITY CLASSIFICATION AUTHORITY			3 DISTRIBUTION/AVAILABILITY OF REPORT APPROVED FOR PUBLIC RELEASE. DISTRIBUTION IS UNLIMITED.			
2b DECLASSIFICATION/DOWNGRADING SCHEDULE						
4 PERFORMING ORGANIZATION REPORT NUMBER(S) WESTINGHOUSE-O/NPT-723-HYDRO-CR-88-01			5 MONITORING ORGANIZATION REPORT NUMBER(S)			
6a NAME OF PERFORMING ORGANIZATION Westinghouse Oceanic Division Cleveland Operations		6b OFFICE SYMBOL (if applicable)	7a NAME OF MONITORING ORGANIZATION DCASPRO- Westinghouse			
6c ADDRESS (City, State, and ZIP Code) Hydrothermodynamics Research and Technology One Corporate Place Middletown, RI 02840			7b ADDRESS (City, State, and ZIP Code) c/o Westinghouse Oceanic Division 18901 Euclid Avenue Cleveland, Ohio 44117-0668			
8a NAME OF FUNDING/SPONSORING ORGANIZATION Office of Naval Research		8b OFFICE SYMBOL (if applicable) Code 1131M	9 PROCUREMENT INSTRUMENT IDENTIFICATION NUMBER N00014-87-C-0668			
8c ADDRESS (City, State, and ZIP Code) 800 N. Quincy Street Arlington, VA 22217			10 SOURCE OF FUNDING NUMBERS			
			PROGRAM ELEMENT NO	PROJECT NO	TASK	WORK UNIT ACCESSION NO
11 TITLE (Include Security Classification) Metal Transfer in Gas Metal Arc Welding						
12 PERSONAL AUTHOR(S) Donald M. McEligot and James S. Uhlman, Jr.						
13a TYPE OF REPORT Final Report		13b TIME COVERED FROM 18 Sep87 to 17 Mar88		14 DATE OF REPORT (Year, Month, Day) 1988 March 17		15 PAGE COUNT
16 SUPPLEMENTARY NOTATION						
17 COSATI CODES			18 SUBJECT TERMS (Continue on reverse if necessary and identify by block number) Welding, GMAW, Heat transfer, Metal transfer, Droplet, Detachment, Melting, Numerical predictions. (JIS)			
FIELD	GROUP	SUB-GROUP				
19 ABSTRACT (Continue on reverse if necessary and identify by block number) The ultimate goal of the present work is to develop sufficient fundamental understanding of generic GMA welding to enable prediction of the weld quality to be made in terms of the material properties and control parameters. Evidence from experiments and simple analyses shows that the melting rate is controlled by the thermofluidmechanic behavior of the molten electrode tip. Consequently, an analytical and numerical study of the transient, thermofluidmechanic behavior of the detachment phase for metal transfer in GMA welding has been initiated. The present report, for the first half year of the study, reviews the related background and then concentrates on approximate length and time scales analyses preparatory to the development of a transient, axisymmetric numerical analysis to describe droplet detachment in globular and spray modes. To date these analyses have not revealed any significant simplifications which would be useful for the governing partial differential equations. The numerical approach in process is outlined briefly.						
20 DISTRIBUTION/AVAILABILITY OF ABSTRACT <input checked="" type="checkbox"/> UNCLASSIFIED/UNLIMITED <input checked="" type="checkbox"/> SAME AS RPT <input type="checkbox"/> DTIC USERS			21 ABSTRACT SECURITY CLASSIFICATION Unclassified			
22a NAME OF RESPONSIBLE INDIVIDUAL Dr. Ralph W. Judy			22b TELEPHONE (include Area Code) (202)696-4402		22c OFFICE SYMBOL Code 1131M	

TABLE OF CONTENTS

SECTION	PAGE
ABSTRACTii
LIST OF FIGURESiv
NOMENCLATURE	v
1. INTRODUCTION1
1.1 Background1
1.2 Goal2
1.3 Droplet phenomena2
1.4 General problem4
1.5 Related work5
1.6 Approach10
2. PRELIMINARY RESULTS	14
2.1 Typical magnitudes.	14
2.2 Steady radial temperature variation	15
2.3 Axial temperature gradient.	15
2.4 Thermocapillary ("Marangoni") convection	16
2.5 Time scales - gas	17
2.6 Time scales - droplet	18
3. NUMERICAL TECHNIQUE	24
3.1 Background	24
3.2 General approach	26
3.3 Status.	31
4. CONCLUDING REMARKS AND RECOMMENDED PLANS	31
TABLE 1. Approximate Thermofluid Properties of Mild Steel and/or Iron [Waszink and Piena, 1985]	33

FIGURES

REFERENCES CITED

LIST OF FIGURES

FIGURE	TITLE
1.	Schematic description of control parameters in gas metal arc (GMA) welding
2.	Range of metal transfer according to length of wire per drop [Needham and Carter, 1965]
3.	Thermal processes in an idealized, vertical droplet
4.	Effect of current on the size and frequency of drops transferred from a 1-1/2 mm (1/16 inch) steel electrode in an argon shielded arc [Lesnewich, 1958b]
5.	Illustrative example of adaptive, curvilinear finite-control-volume grid for detachment process of metal transfer in gas metal arc welding
6.	Numerical prediction of bubble growth at a wall under the influence of gravity and surface tension [Meng and Uhlman, 1986]
7.	Typical grid scheme in early stage of development
8.	Mesh and control volumes in staggered grid

NOMENCLATURE

A_{CS}	Cross-sectional area
A_S	Surface area
C	Solute (additive) concentration
C_p	Specific heat at constant pressure
D, d	Diameter
E	Electric field strength
\bar{F}	Overall grey-body radiation factor
G	Average mass flux, \dot{m}/A_{CS}
Gr	Grashof number, $\rho_i^2 g D^4 q_w'' / (\mu^2 k_i T_i)$
g	Acceleration of gravity
g_c	Unit conversion factor
H	Magnetic field strength
h	Convective heat transfer coefficient, $q_w'' / (T_w - T_b)$
K_S	Solute (additive) diffusivity
k	Thermal conductivity
\dot{m}	Mass flow rate
Nu	Nusselt number, hD/k
p	Static pressure
Pr	Prandtl number, $c_p \mu / k$
q	Heat transfer rate; electronic charge
q^+	Heating rate parameter, $q_w'' / (Gc_p T_i)$
q_w''	Wall heat flux
Re	Reynolds number, $4\dot{m} / (\pi D \mu)$
St	Stanton number, h / Gc_p
T	Absolute temperature

NOMENCLATURE - Continued

t Time; relative temperature (e.g., °C)
u Velocity component
v Voltage; V_e , electrode (wire) feed velocity
x Axial distance

Greek letters

ϵ_s Surface emissivity
 μ Viscosity; μ_m , magnetic permeability
 ρ Density
 σ Surface tension; Stefan-Boltzmann constant
 σ_e Electrical conductivity

Subscripts

i Evaluated at inlet bulk temperature
r Radiative
s,w Evaluated at surface conditions
 ∞ Evaluated at freestream conditions

METAL TRANSFER IN GAS METAL ARC WELDING

1. INTRODUCTION

1.1 Background

Gas metal arc (GMA) welding is the major method for welding steels, superalloys and aluminum; about 30 to 40 percent of the production welding in this country is accomplished by this process. In naval ship construction a greater percentage of the welding is by GMA, and more will be necessary for HY-100 and HY-130. Yet the behavior of the interacting physical phenomena, which determine the weld quality in this complicated process, are not yet understood well.

GMA welding is important in the construction of Naval ships and submersibles. In particular, the operating depth of submersibles can be increased by a factor of two by using titanium alloys [Masubuchi and Terai, 1976] if reliable welds can be insured. The gas tungsten arc (GTA) process has proved to be reliable but slow. In order to be used in a production shipyard environment, automatic and manual all-position GMA processes need to be developed for titanium. Data by Ries [1983] show that pulsed current GMA welding should provide a reasonable large scale production technique for joining large titanium structures.

A typical GMA welding process is described schematically in terms of some physical parameters controlling the welding process in Figure 1. Three coupled regions are important in the formation of the weld: the molten weld pool, the plasma arc and the molten droplet region at the tip of the traveling (wire) electrode. The droplet region provides the weld filler metal which is transferred through the arc to the weld pool. One of the major obstacles in making a good GMA weld is controlling the metal transfer process so that the molten filler metal is incorporated in the weld pool in a controlled, calm, and orderly fashion. This detachment rate then determines the rate at which the GMA torch can be moved in the direction of the desired weld, i.e., the welding rate.

Tests by AirCo approximately three decades ago showed that various additives on the surface of welding rods could cause significant variations in the deposition rate [Cameron and Baeslack, 1956]. One likely effect of such additives would be a modification of the surface tension of the liquid metal in the droplet. In comparable experiments with GTA weld pools, Heiple and Roper [1982] demonstrated that such alteration of surface tension gradients changed the fluid flow patterns and the fusion zone geometry significantly. Thus, it is anticipated that surface-tension-driven flow ("Marangoni convection") [Levich and Krylov, 1969; Ostrach, 1977, 1983] induced by temperature gradients in the molten droplet will also have a significant effect on the droplet formation, flow and detachment and, therefore, on the metal transfer rate.

Sunmewa and Mucolu [1985] in Japan have shown that the electrode wire melting rate can also be increased by increasing the ambient pressure at which the GMA operation is conducted. The basic phenomena accounting for this increase have not been identified.

From experiments and simple analyses at Philips Research Laboratories, Waszink and Piena [1985] concluded that, for covered electrodes, the melting rate is controlled by electromagnetically-induced fluid flow in the electrode tip. However, they estimated that for the conditions of their experiments surface tension forces and buoyancy forces were of the same order-of-magnitude as electromagnetic forces, i.e., 1:1:3. Therefore, since they consider convection in the droplet to be important in the detachment process, we propose to conduct an analytical and numerical study of the transient thermalfluidmechanic behavior of this process in GMA and to examine the validity of the results by comparison to measurements at DTRC and MIT. Both "steady" and pulsed operation would be studied.

1.2 Goal

The general goal is to develop sufficient fundamental understanding of generic GMA welding to enable prediction of the weld quality to be made in terms of the material properties and control parameters for metals and alloys important in practical situations. Accomplishment of this goal ultimately requires understanding of the weld pool, plasma and droplet regions and their interactions.

The immediate objective of the proposed work is to develop the necessary basic knowledge of the thermalfluidmechanical behavior of the droplet region or electrode tip.

Potential consequences of this knowledge are controllable increases in melting or welding rate, understanding of the mechanism of transition from subthreshold to "normal mode" of droplet detachment, reduction of spatter, quantitative evaluation of present qualitative hypotheses, reduction of smoke or fume formation, etc. In addition, if the mechanism of enhanced electrode melting rate experienced by Cameron and Baeslack (and others since then) could be understood and controlled, it would permit up to 20 or 30 percent increases in GMA weld productivity. If this is accomplished at essentially the same welding heat input, it would permit welding of higher strength materials which are ordinarily degraded by current arc welding processes. Such gains in productivity and weldability of advanced materials would have tremendous economic impact.

1.3 Droplet Phenomena

The detachment process can be characterized and related to weld quality in a number of ways. Forces involved include gravity, induced electro-magnetic (Lorentz) forces, surface tension, internal pressure, hydrodynamic drag, plasma arc reaction or impingement and electrostatic forces.

Cooksey and Miller [1962] describe six modes of metal transfer as follows:

1. Large drops detach with little influence of arc forces. The controlling forces are gravity and droplet surface tension.
2. The drop remains spherical under surface tension forces but is detached from the electrode before gravity transfer occurs by additional force provided by the electrode plasma and Lorentz pinching forces.
3. The drop is distorted, lifted and repelled from the plate as a result of arc forces. The net repelling force comes from either Lorentz forces in the drop in an off axial direction due to anode or cathode spot instability or plasma jets from the weld pool where high current densities are concentrated at anode or cathode spots.
4. The end of the electrode is tapered and a fine spray of drops stream off due to well developed plasma jets and Lorentz pinching forces.
5. Molten metal from the electrode tip streams off in an upward direction as a result of reaction forces from metal vapor streams in plasma jets from the droplet to the weld pool or vice versa.
6. The molten metal drop and arc move sideways while the neck attaching the drop to the electrode is thrust in the opposite direction. The curvature of the current path caused by drop and arc movement gives a sideways Lorentz force and as the neck moves, the curvature, and hence the magnitude of the force, increases until separation occurs.

Cooksey and Miller indicate that the actual metal transfer for a given material can be a combination of any of the above modes depending upon the magnitude of the forces effecting metal transfer.

Ries [1983] indicates that the ideal type of transfer incorporates a balance of droplet ejecting and repelling forces such that droplet sizes on the order of the diameter of the electrode are formed and transferred with minimal acceleration to minimize weld pool turbulence. Needham [1962] describes two modes of metal transfer in GMA welding on aluminum:

1. Normal - Rapid spray transfer of small drops on the order of the electrode diameter (most desirable mode).
2. Subthreshold - Infrequent transfer of large globules (used sometimes for short circuiting transfer).

Since these two modes represent two different weld bead formation modes with varying penetration, the inadvertent change from one mode to another caused by only small changes in current, can have a devastating effect on weld quality. A current change of about 25 amps at 250 amps can cause an abrupt transition from the subthreshold mode to normal mode; the reason for this transition is not understood.

To quantify the mode of transfer occurring throughout the normal and subthreshold ranges better, Needham and Carter [1965] define the ranges of metal transfer according to the length of wire per droplet (Figure 2). According to Lancaster [1962], subthreshold transfer for aluminum occurs by gravity with the droplet temperature well below boiling whereas spray transfer occurs by injection of the droplet into the arc stream by pinch forces at temperatures ranging from the melting point during drop formation to the boiling point before transfer.

1.4 General problem

The thermal processes which interact with the forces on the droplet to cause detachment are described schematically in Figure 3 for an idealized droplet. The process is transient, possibly periodic, proceeding from detachment of one droplet through melting, formation and detachment of the next, so there is a change in the thermal energy storage S . Heating is caused by electrical resistance heating (or possibly induction) G and by interaction with the plasma q_p . Heat losses occur via conduction in the solid rod q_k , radiation exchange with the environment q_r , convection to the shielding gas q_c and possible evaporation at the surface q_v . Internal circulation q_{nc} is induced by electromagnetic, surface tension, gravity and shear forces.

Whether the smallest sized droplets are caused by minute fluctuations on the surface of the larger molten tip, possibly induced by Taylor or shear instabilities, or whether caused by condensation and agglomeration of metal after its evaporation at the surface is not clear. Understanding this problem is important in developing methods to control fume formation (a health hazard) on one hand and controlling spatter on the other.

For the droplet region, the general mathematical description is provided by the governing partial differential equations,

Momentum,

$$\rho \frac{D\vec{u}}{Dt} = -\nabla p + \rho \vec{g} + \rho_e \vec{E} + \mu_m \vec{J} \times \vec{H} + \nabla \cdot (\mu \nabla \vec{u}) \quad (1)$$

Thermal energy,

$$\rho C_p \frac{DT}{Dt} = \nabla \cdot (k \nabla T) + \dot{Q} + \frac{J^2}{\sigma_e} \quad (2)$$

Species (additives),

$$\frac{DC}{Dt} = K_s \nabla^2 C \quad (3)$$

Continuity

$$\nabla \cdot \vec{u} = 0 \quad (4)$$

Maxwell's equations,

$$\nabla \times \vec{E} = - \frac{\partial}{\partial t} (\mu_m \vec{H}) \quad (5)$$

$$\nabla \times \vec{H} = \vec{J} + \frac{\partial (c \vec{E})}{\partial t} \quad (6)$$

$$\nabla \cdot (\mu_m \vec{H}) = 0 \quad (7)$$

$$\nabla \cdot (c \vec{E}) = \rho_e \quad (8)$$

$$\vec{J} = \sigma_e (\vec{E} + \vec{u} \times \mu_m \vec{H}) \quad (9)$$

and property relations plus interface/boundary conditions.

These equations describe an incompressible viscous fluid with a passive solute in gravitational, thermal, electrostatic and magnetic fields. The forces possibly imposed on an internal fluid particle are: pressure gradient, gravity, Lorentz, electrostatic and viscous shear stress. The unknowns are: \vec{u} , p , \vec{H} , \vec{E} , T and species concentration C . The fluid properties can depend on their temperatures and concentrations. There are six unknowns and six equations; therefore, we have a mathematically complete system, but a complicated one.

In the solid rod, which is coupled to the droplet via conditions at the melting interface, the problem is simplified by eliminating the momentum equations (1) and continuity equation (4) from the system of equations since the velocity is zero (relative to the wire feed velocity).

In order to obtain fundamental understanding of the GMA process, it is necessary to simplify these equations to represent only the dominant phenomena. Ultimately, such simplification will also be necessary to develop practical control systems for the actual application.

1.5 Related work

For a general review of recent work in metal transfer, the reader is referred to Lancaster's chapter in the text by Study Group 212 of the International Institute of Welding [Lancaster, 1984]. Numerical studies of the fluid mechanics of the weld pool are being conducted by M. M. Chen and

Mazumder at the University of Illinois, Szekely at MIT [Oreper and Szekely, 1984] and Kou at the University of Wisconsin [Kou and Wang, 1986] and by Carey at the University of Texas using finite difference and finite element techniques, respectively. Other weld pool simulations are underway by Matsunawa at Osaka, Martin-Marietta [Traugott, 1986], Deb Roy at Penn State and Mahir at Lawrence Livermore Laboratory. For over twenty years, Pfender and his students at the University of Minnesota have been studying plasma arcs [Pfender, 1978; Sanders and Pfender, 1984]. Kovitaya and Lowke [1985] have also been developing theoretical models of free burning arcs as in welding.

In measurements on weld pools, Heiple and Roper [1982] found that the presence of low concentrations of surface active impurities can substantially alter the temperature dependence of the surface tension as well as changing its magnitude. These changes vary the fluid flow patterns in the weld pool and change the fusion zone geometry.

At MIT, Eagar is developing a fast "multicolor" pyrometer, with higher spatial and temporal resolution than currently available, to determine local temperatures during transient welding processes. Flow visualization of welding is conducted in his laboratory as well as at Idaho National Engineering Laboratory (M. MacIlwaine and H. Smartt) and David Taylor Research Center. Results from the proposed work would be compared to their measurements. Predictions can also be compared to integral measurements as by Halmoy [1980] for melting rate and by Ueguri, Hara and Komura [1985] for average temperature or average heat content of droplets.

A number of recent studies have provided approximate analyses and experimental results for models of droplet detachment. The classic, pioneering study of metal transfer by Lesnewich [1958 a,b] has been recently summarized by him in a letter [Lesnewich, 1987].

Lesnewich [1958 a] noted the heat for electrode melting is produced simultaneously by the anode or cathode reactions, depending on the polarity and resistance of the welding wire to the flow of current. Only a small portion of the heat is received by radiation from the arc stream or the weld crater. Anode heating is affected by the electrode diameter and the magnitude of welding current. Cathode heating also is dependent upon these factors and, in addition, upon the electrode extension and activation. Electrical-resistance heating is controlled by the electrode extension, diameter and activity, and the current magnitude. The arc length has a measurable effect on resulting rate only in a very few welding applications.

Lesnewich [1958 b] classified metal transfer in gas-shielded welding arcs as either globular or spray, the spray transfer occurring as either axial-spray or rotating-spray. The globular transfer is characteristic in active shielding gases. It also is developed in inert-gas shields with all electrodes using reverse- or straight-polarity direct current when the current is below some critical level (Figure 4). Above this level, which has been termed the transition current, the metal transfer changes suddenly from globular to axial-spray. This transfer is characterized by the movement, in line with the electrode axis, of minute drops of molten metal

from the electrode to the work. It is unique with inert-gas-shielded arc welding and can be achieved with all electrodes when operated with reverse-polarity direct current. With emissive-agent-coated electrodes it can be achieved using straight- or reverse-polarity direct current or alternating current. At some higher level of welding current, the spray of metal suddenly ceases to be transferred in line with the electrode. Its axis begins to rotate rapidly so as to form a conical surface of revolution with its apex at the tip of the electrode. The angle at the apex increases with increasing currents and can cause the development of considerable weld spatter.

The axial-spray transfer is preferred for gas-shielded metal-arc welding to insure maximum arc stability and minimum spatter. Lesnewich [1958 b] discusses the factors that affect the transition at some current level from globular to axial-spray transfer and, at some higher currents, from axial-spray to a rotating-spray transfer.

The lower transition current is affected by the composition of the electrode and the degree of electrode activation; this is true with both straight- and reverse-polarity direct-current arcs in inert-gas shields. The transition current can be decreased by reducing the electrode diameter or increasing the length of the electrode that extends from the current contact.

The current for transition to rotating-spray transfer also is dependent upon the electrode composition, the electrode extension and the electrode diameter. With straight-polarity direct current, it is affected by the amount and type of emissive-agent coating on the electrode surface. Lesnewich [1958 b] discusses the influence of these effects upon the selection of current, electrode extension, electrode diameter and activation to achieve a particular electrode melting rate and type of transfer.

Greene [1960] developed approximate analyses for formation and transfer of drops under the influence of (1) gravitational forces and surface tension, (2) arc forces and surface tension and (3) all three forces. It was assumed that the current density at the active surface is uniform and remains constant with changes in current. Transfer was characterized by two dimensionless parameters: drop size index and transfer number.

Halmoy [1980] calculated the ohmic heating in the electrode extension of different filler wires exactly for real values of resistivity and specific heat, using a simple technique of graphical integration, yielding the distributions of heat content and voltage along the wire. A simple method to measure the ohmic heating of any wire directly was also tested. For normal MIG-welding the ohmic heating increases linearly with the extension. Adding the effect of anode heating, Halmoy established a simple equation for the melting rate. The melting rate depends on the droplet temperature and the effective melting potential. Melting rates as a function of extension and current were measured. Comparison with the calculations shows that the detaching droplets are heated only slightly above the melting point. The effective anode melting potential was essentially equal to or less than the electron work function, which implies that the melting rate is largely unaffected by the shielding gas.

Woods [1980] studied metal transfer while welding aluminum by the GMAW process. Particular attention was paid to the role of high vapor pressure alloying elements in determining the mode of metal transfer. It was shown that the transfer characteristics of all alloyed filler metal wires depend upon the concentration of high vapor pressure alloying elements incorporated in the wire. The presence of a high vapor pressure element causes breakdown in the stability of metal transfer, which in turn results in a high level of spatter formation. Such behavior is normally found when welding with the 5000 series or magnesium-containing aluminum filler alloys. Explosive phenomena occurring during metal transfer have indicated that the average temperature of droplets during transfer is approximately 1700°C (3092°F). This agrees well with calculations based upon heat input and electrode burnoff considerations.

During the last several years, Waszink and co-workers have presented a series of approximate analyses and experiments dealing with metal transfer. Waszink and van den Heuvel [1982] investigated the physical processes governing the generation and the flow of heat in a consumable mild steel wire to determine the influence of the welding parameters on melting rate and drop temperature. The work was limited to processes where the wire is at positive polarity. The analysis of the heat balance was based on measurements of the melting rate as a function of the electric current and the extension length, at a given wire diameter.

The ohmic power developed in the wire was calculated from the measured data. It was found that it is, in general, not sufficient to account for the observed melting rate. Consequently, there must be a flow of heat from the anode surface on the molten tip, through the liquid metal, to the solid part of the wire. The corresponding heat flow rate was derived from the experimental data; it was found to depend on current and melting rate.

Simple physical models were presented that describe the transport of heat through the liquid and account for the experimental results. In the model for globular drop transfer, the dominant mechanism is fluid flow, which is caused by the Lorentz force. In the case of spray transfer, the heat flow is ascribed to thermal conduction through the liquid metal that is flowing down the pointed wire tip. The models yield expressions for melting rate and drop temperature as functions of current, extension length, and wire diameter.

An analysis was made of data reported by Lesnewich on the critical current for the transition from globular to spray transfer. This transition occurs in a current range where the downward force on a drop is mainly due to the impact of the incoming liquid, and to electromagnetic effects. It was found that the total downward force is roughly equal to the sustaining force by the surface tension, at the critical current.

Waszink and Graat [1983] carried out experiments in a welding arc having a consumable wire as the positive electrode. The drop mass was measured as a function of the gas flow rate and the electric current. The electrode was surrounded by a hot plasma, so that measurements at zero electrode current could also be made. The various forces acting on a drop at the point of detachment were derived from the measured data.

The following forces were considered: gravity force, the force exerted by the flowing gas, electromagnetic force, and the surface tension force by the surface tension. The model which was used in the derivation of these forces is based on older work on drop transfer from capillary tubes. The Lorentz force due to the divergence of the electric current within the drop accounted for the electromagnetic force as derived from the measured data.

Allum [1985 a] considered, largely in the context of metal transfer in arc welding, the stability of a viscous, current-carrying fluid cylinder with surface charge. Simple expressions were obtained between the characteristics of instability growth and the dependence of these on process parameters. For liquid metals considered it was found that viscous effects are negligible while electrostatic effects exert a stabilizing influence and may have a number of interesting effects on stability (particularly at low wire currents). Allum [1985 b] then developed a model of metal transfer in open arc welding which provides a framework for predicting the influence of welding parameters in steady and pulsed current welding. It was found possible to present results in terms of simple expressions which are in broad agreement with available observations. Considered were aspects such as droplet evolution, detachment frequency and size, selection of pulse parameters, influence of electrostatic stress on transfer, drop dynamics and the relationship between balance of force approaches to transfer and the present instability model.

Waszink and Piena [1986] measured the velocity of drops detached from a consumable wire during GMA welding and the diameter of the drop neck during the detachment process with the aid of high-speed photography. Wire materials were mild steel, AlMg5 and AISi5. Most of the measurements were made with a pulsed current; drop transfer was of the globular type. It was found that the pendent drop contracts when the pulse starts and that it becomes unstable when its diameter reaches a certain critical value. The velocity at detachment from mild steel wire can be ascribed to electromagnetic forces acting after the drop has become unstable. Another additional mechanism must be operative when the wire material is one of the aluminum alloys. This mechanism was not identified with certainty. The acceleration of the drops in the arc after detachment can be ascribed to a gradient in the plasma pressure, also caused by electromagnetic effects. Analysis of the heat balance indicates that the drop temperature is lower in pulsed welding than it is in welding at a constant current.

Waszink and Piena [1985] applied a steady, one-dimensional analysis to the electrode tip of covered electrodes used for shielded metal arc (SMA) welding. In order to solve the problem, they hypothesized that the effect of metal evaporation was negligible but, by comparison to their experiments, they concluded this idealization was incorrect. They also found differences between covered and bare electrodes but were unable to explain them. For the conditions of their experiments, they determined that convection was important with electromagnetic forces being the largest contributor. However, buoyancy- and surface tension driven-forces were not negligible.

Working with Eagar, Ries [1983] reviewed the principles and experience with pulsed GMA and conducted approximate analyses of the forces involved. He developed a high-speed photographic technique to observe the process of

weld metal transfer and conducted titanium bead-on-plate welding experiments with pulsed current. As a consequence, he concluded that controllable weld metal transfer may become feasible for titanium using pulsed current GMA welding.

A number of general purpose, fluid mechanics codes are becoming available commercially and from the National Laboratories; versions are available in two and three-dimensions, steady and transient, with variable properties, free surfaces, multiple phases, etc. [McEligot, 1985]. Comparable to the present problem in many ways are the numerical solutions developed for treating the "reverse" problem of crystal growth [Langlois, 1985]. For example, for Czochralski growth of silicon, the predictions must include phase change, buoyancy, magnetic fields, surface tension forces, electrical resistance heating, axisymmetry and unsteadiness as well as rotation. These are also problems with multiple length scales; one consequence is that flow sub-regions (layers or cells) can occur but be missed in numerical studies if the resolution is not sufficiently good [Ostrach, 1982]. One important difference is that in the normal metal transfer problem the magnetic field is induced whereas in crystal growth by the Czochralski process it is imposed externally [Kohda et al., 1985]. However, use of an external magnetic field for GMA welding is being investigated by Eagar and his students.

1.6 Approach

To develop basic understanding and predictive procedures for the thermal-fluidmechanical behavior of the detachment phase for metal transfer in GMA welding, preliminary approximate studies and time/length scale analyses are being applied, and numerical prediction techniques are being developed. It is expected that the results will be compared to the related measurements of Prof. T. W. Eagar, MIT, and of DTRC .

The general goal and objective have been described above. The initial problem attacked is the transient behavior of the molten and solid regions for a vertical configuration under an axisymmetric idealization.

The analytic and numerical study concentrates primarily on prediction of the behavior within the droplet.

1.6.1 Task a. Approximate analyses. Approximate analyses of the transient thermal phenomena will be conducted to extend the study of the orders-of-magnitude of the forces as estimated by Ries [1985] and others. Phenomena to be considered include radiation and convection from the solid and the molten drop, conduction, internal circulation, change of phase by melting and vaporization, heating from the plasma and transient energy storage and energy generation as indicated in Figure 3. The purpose of these analyses will be to identify the dominant phenomena during the droplet growth to permit simplifying the complicated mathematical problem.

In this phase orders-of-magnitude will be estimated via empirical correlations and one-dimensional (spherical or cylindrical) approximations.

For example, for cases where the residence time of the shielding gas is short compared to the droplet period (quasi-steady idealization), forced convection from the droplet will be estimated via Newton's law of cooling,

$$q_w'' = h (t_s = t_\infty)$$

and an empirical correlation for the Nusselt number for a sphere. A grey body approximation will be employed for radiation,

$$q_r = \int_s \rightarrow \infty A_s \sigma (T_s^4 - T_\infty^4) \approx \epsilon_s A_s \sigma (T_s^4 - T_\infty^4)$$

where surface emissivity ϵ_s may be estimated from Eagar's measurements. Extended surface theory can be adapted to the solid electrode to predict q_k provided the Biot number, hD/k_{solid} , is low enough. Comparable approximations will be applied to evaluate the other terms.

1.6.2 Task b. Time, length and velocity scales. Simple analyses are employed to identify appropriate velocity, length and time scales and to discover the likelihood of flow subregimes, such as shear layers, internal boundary layers, etc. [Ostrach, 1982]. The time scale analyses are used to identify which aspects of the transient problem can be treated as quasi-steady and which will require full non-steady analysis. The length scale results also aid in finding the proper resolution for the variably-spaced mesh used in the numerical analysis.

1.6.3 Task c. Simplification. The results of tasks (a) and (b) are employed to simplify the mathematical statement of the problem in order to reduce computer time and storage required and to ease understanding of the numerical results of task (d).

1.6.4 Task d. Numerical technique. This task develops the numerical technique(s) to solve the problem. While the results of task (c) are required in order to identify the character of the system of governing partial differential equations to be solved, it is anticipated that the droplet region will be represented by a parabolic system of equations, due to the time-dependence, with two significant spatial dimensions. Away from the melting interface, the transient distributions in the solid electrode can be expected to reduce to a single dominant spatial variation.

Typical boundary conditions at the melting interface between the solid electrode and the molten droplet are:

- . Velocities equal electrode feed velocity
- . Continuous temperature
- . Energy balance between heat fluxes and energy required for heat of fusion
- . Mass fluxes of species are continuous
- . Magnetic field and electrical field are continuous.

At the outer surface of the solid electrode they are:

- . Energy balance between heat fluxes and thermal radiation
- . Negligible species mass transfer

- . Negligible electrical conduction in radial direction
- . Magnetic field to be related to externally applied field (which may be zero).

At the liquid metal surface the first boundary conditions used would be:

- . Energy balance between conduction, convection, radiation, energy absorbed from plasma arc and energy required for heat of vaporization (if any)
- . Balance of mass fluxes of individual species
- . Force balances accounting for effect of surface tension with surface curvature plus drag of shielding gas
- . Specified distribution for magnetic and electrical fields.

The boundary conditions on the liquid surface are to be the most uncertain, at first, since they are coupled to the plasma arc behavior around the bottom of the droplet region. In order to develop the numerical procedure, the first calculations will employ plausible distributions estimated in consultation with Professor Eagar. As the study proceeds and more understanding of the arc behavior becomes available, the treatment of these conditions will be improved. Coupled solutions for the interaction of the plasma arc with the droplet are mentioned later as a logical further extension.

Radiation from the arc will be included in the thermal boundary condition at the liquid metal surface, partly for later extensions. Despite the high temperature of the arc it is expected to be a small contribution relative to other energy transfer from the arc, and the view factor to the highest temperature region will be small. Sensitivity to this distribution can be tested easily by varying the parameters.

Droplet detachment is expected to be a near-periodic process, with or without pulsed power supplies. At first, calculations may be conducted from an assumed initial state through successive cycles of detachment to deduce the natural period and the distributions as functions of the temporal phase. This calculation would be without a pulsed source in order to avoid confusion from a possible beat frequency arising from two different frequencies: natural and imposed.

The initial state chosen may be (a) a cold, fresh electrode, (2) an estimate of the shape of the molten electrode tip immediately after detachment plus estimates of the distributions of the dependent variables or (3) an arbitrary state differing significantly from (1) or (2). The first could give a description of the start-up process while the second is expected to aid convergence to the periodic solution, particularly as experience is accumulated. Comparison of results from initial conditions (1), (2) and (3) will provide insight into the dependence on the choice of initial condition and, in conjunction with the time scales analysis, indications of the response time of the system.

To our knowledge, there is no 'canned', general fluid mechanics code available that would handle the problem posed. Existing programs, which have some desirable features relevant to the thermofluids part of the

problem, are being used for guidance to expedite the initial progress and to avoid "re-inventing the wheel." An inexpensive, plausible beginning is described below as an example. Substantial extensions and modifications will be required. The determination of the most important directions in which these developments should proceed will be among the results of approximate analyses referred to as task (a).

While there are a variety of general purpose fluids codes available [McEligot, 1985] it is anticipated that solutions will be obtained by developing an axisymmetric version of a code comparable to the inexpensive TEAM code of Prof. B.E. Launder and Dr. M.A. Leschziner of UMIST [Huang and Leschziner, 1983]. For example, the TEAM series uses a finite-control-volume technique for heat, mass and momentum transfer in laminar and turbulent flows with forced or free convection. Convective terms are modeled by the QUICK algorithm of Leonard [1979; Huang, Launder and Leschziner, 1985] to reduce numerical diffusion and to obtain more accurate solutions than with standard upwind differencing while maintaining numerical stability. Pressure-velocity iteration is accomplished by employing an adapted version of the SIMPLER algorithm [Patankar, 1980] to speed convergence; revision to the SIMPLEX method [van Doormaal and Raithby, 1985] is under consideration. Near surfaces or interfaces a parabolic (equation) sublayer model may be employed for energy and momentum transfer in order to reduce the number of nodes at which the time-consuming pressure calculation must be conducted while maintaining accuracy in regions with steep gradients.

Coarse, curvilinear grids may be used to approximate the geometry at first and then would be refined where needed; Figure 5 illustrates the features of possible grid schemes. Variable node spacing will be employed in order to improve accuracy in regions of high gradients. As the droplet grows, varying the size and shape of the various regions, the grid will be redistributed and the locations of the free surface and interfaces may be determined following concepts as in the LINC code, developed at Los Alamos to treat free surface problems.

As noted above, in the solid electrode the fluid mechanics solution will be suppressed. An enclosure treatment may be used to interrelate the radiating surface boundary conditions around the electrode.

The use of the TEAM technique provides an implicit or semi-implicit approach in the time coordinate so the time intervals Δt are not as limited as with an explicit technique. Typical revisions of such a code would include readjustment of the grid shape with time, provision for deformable interfaces and free surfaces, and addition of equations to treat the magnetic and electric fields.

The governing equations are essentially the same in the solid interface/ boundary layer region, but a separate calculation may be made concentrating more nodes--to obtain greater detail--in the vicinity. Alternatively, approximate closed-form analyses may be employed for these and other boundary regions. The time scales analyses should determine to what extent this part of the problem can be considered quasi-steady. It is anticipated that boundary layer approximations will be valid in this region once the

bulk flow in the droplet has been determined. The potential of including this part of the problem as an extension of a parabolic sublayer treatment in the overall problem will also be considered.

While some of the terms in equations 1 through 6 (which were presented partly to demonstrate the complexity of the problem) represent constant fluid properties, the numerical technique will not be constrained to that assumption. This is implied by the mention of property relations and/or temperature dependence. Using finite control volume formulations, as anticipated, eases the difficulty of accounting for property variation. However, some calculations will be conducted with properties held constant in order to isolate effects due to other phenomena. (And in some applications the temperature dependence of the properties is not known well enough to warrant consideration.)

Computer program development will be done using Westinghouse facilities which include VAX 11/8600 and VAX 11/780 super-mini-computers. For more detailed calculations, it is anticipated that a main-frame computer (e.g., CDC7600, CRAY-1XMP, etc.) will be required.

As the computer program is developed it will be compared to appropriate analyses and experiments to test that the individual phenomena are modeled properly. For example, input parameters can be adjusted to yield limiting cases for comparison to simple closed form analyses such as pure conduction, thermal radiation in an enclosure with three isothermal walls, heat transfer from extended surfaces, surface tension determination, etc.

1.6.5 Task e. Comparison. After verification that the computer program performs properly in known cases, calculations will be conducted for comparison to available measurements at DTRC and MIT.

Results will be the predicted transient distributions of the dependent variables, detachment frequencies, droplet sizes and shapes, metal transfer rates, etc.

2. PRELIMINARY RESULTS

2.1 Typical magnitudes

In applications for steel, typical wire diameters are in the range 0.8 to 2 mm (0.03 to 0.09 in.) and wire speeds are of the order 0.04 to 0.1 m/sec (100 to 300 in./min). Shielding gas flow rates are approximately 1.1 to 1.4 m³/hr (40 to 50 ft³/hr) at atmospheric pressure, passing through an annular opening formed between the nozzle and the contact tube with diameters of about 6 and 30 mm (1/4 in. and 1 in.), respectively. The wire "stick out" is about 10 to 30 mm (1/2 to 1 in.) [Eagar, 1987]. Typical thermofluid properties of steel (or iron) in solid and liquid phases are given in Table 1 [Greene, 1960; Waszink and Piena, 1985].

For 1.6 mm (1/16 in.) diameter mild steel, Lesnewich (1958b) shows droplet detachment frequencies to be of the order of 15 per second for currents below 240 amp and 250-300 per second above 280 amp. These values represent globular and spray metal transfer and correspond to periods of about 70 ms and 3 ms, respectively.

The Reynolds number of the droplet, based on wire diameter and feed rate and liquid metal viscosity, is of the order of 100 for steel. Even if a no-slip condition were applied at the surface as in duct flow, one would expect the flow to be laminar. But, since the liquid surface is not constrained, the shear stresses are expected to be much less, so there is more reason to believe the circulation within the droplet to be laminar, if not even so-called creep flow.

The welding gun is normally designed with the intent of providing a laminar flow of the shielding gas around the wire, droplet, etc. to avoid mixing with the surrounding air. The Reynolds number of the gas flow through the nozzle is of the order of 1500. Therefore, the gas flow is not expected to induce turbulent flow in the droplet either.

2.2 Steady radial temperature variation

In the wire the limiting radial variation of the temperature with uniform resistive heating would be given by the asymptotic, steady, one-dimensional solution [Kreith, 1973]

$$T_c - T_o = \frac{i^2 \rho_e r_o^2}{4k A_{cs}}$$

This result would correspond to slow motion of the wire and must be coupled to the external environment by convection and radiation to yield predicted internal temperatures. It implies that all thermal energy is lost radially to the surroundings. Thus, it represents an upper bound rather than practical operation in gas metal arc welding.

2.3 Axial temperature gradient

To estimate the order-of-magnitude of the surface tension gradient, which is a function of temperature, we estimate the axial temperature gradient for a steady, one-dimensional flow. An energy balance without heat loss gives

$$\dot{m} c_p \frac{dt}{dx} = i^2 R' = \frac{i^2}{A_{cs}} \rho_e$$

where ρ_e is the electrical resistivity. Rearrangement and evaluation of the mass flow rate, $\dot{m} = \rho_w v_w A_w$, yields

$$\frac{dt}{dx} = \frac{i^2 \rho_e}{\dot{m} c_p A_{cs}} = \frac{i^2 \rho_e}{\rho_w c_p v_w A_w A_{cs}}$$

Near the solid region $A_{cs} \approx A_w$, giving a dependence on d^4 . As droplets form and are accelerated by gravity or electromagnetic forces, \dot{m} will change locally and the steady flow idealization becomes weak.

2.4 Thermocapillary ("Marangoni") convection

Surface tension generally depends on temperature, composition and electrical potential. Lai, Ostrach and Kamotani [1985] have examined the role of free-surface deformation in unsteady thermocapillary flow for thin liquid layers and rectangular liquid pools. While these geometries differ from liquid droplets, their results should provide order-of-magnitude estimates for the present problem. Further, for short times when the motion is still confined to a thin region near the surface, the results for the dissimilar geometries should approach each other; i.e., both cases should be effectively two-dimensional, semi-infinite situations.

The importance of thermocapillary convection can be estimated from a number of non-dimensional parameters:

- 1) "Static bond number"

$$Bd = \frac{\rho g L^2}{\sigma}$$

hydrostatic effects relative
to surface curvature effects
on pressure

- 2) "Elevation Bond number"

$$Bo = \frac{\rho g D^2}{|\partial\sigma/\partial T| \Delta T}$$

hydrostatic pressure
thermocapillary dynamic pressure

- 3) "Dynamic Bond number"

$$Bo_d = \frac{\rho \epsilon D^2 \beta}{|\partial\sigma/\partial T|}$$

natural convection
thermocapillary convection

Additional related parameters are

$$\text{Surface-tension Reynolds number, } Re_\sigma = \frac{D |\partial\sigma/\partial T| \Delta T}{\mu \nu}$$

$$\text{Marangoni number, } Ma = Pr Re_\sigma$$

$$\text{Capillary number, } Ca = A \frac{|\partial\sigma/\partial T| \Delta T}{\sigma} = A^3 \frac{Bd}{Bo}$$

where A is the aspect ratio, D/L, of the liquid layer. For order-of-magnitude calculations we interpret L as half the drop circumference.

To estimate values of these parameters for a liquid steel droplet, we take the temperature range as being from the melting point to a maximum about 500K below the boiling point [Oreper, Eagar and Szekely, 1983].

Following Waszink and Graat [1983], we took surface tension values for mild steel to be dominated by the manganese constituent with $\sigma \approx 0.9$ N/m (0.005 lbf/in) and $|\partial\sigma/\partial T| \approx 0.2 \times 10^{-3}$ N/mK (6×10^{-7} lbf/in F). The capillary number for these values is about 0.2A.

Estimated magnitudes of the parameters become

	<u>Bd</u>	<u>Bo</u>	<u>Bo_d</u>
Globular	2	10	0.8
Spray	0.2	1	0.08

With the exception of Bo for globular transfer and Bo_d for spray transfer, these parameters are all of order one. For globular transfer hydrostatic pressure would be expected to be significantly greater than the thermocapillary dynamic pressure. And for spray-sized droplets, Marangoni convection would be significantly greater than natural convection.

The value of Bd \approx 0.2 for spray transfer would be an indication that a force(s) other than gravity is involved in droplet detachment in that mode, since surface curvature would cause greater pressure (and restoring force) than the weight of the drop. Greene [1960] and Waszink and Piena [1985] have concluded from different arguments that the additional forces are electromagnetic and, therefore, Maxwell's equations should be included in the solution.

While thermocapillary convection is indicated to be as important or more important than natural convection (Bo_d \approx 1), it is not immediately clear that either is significant since both are propagated by viscous effects. Unsteady considerations are necessary to estimate whether they are negligible or dominant in the droplet growth.

2.5 Time scales - gas

The shielding gas flow provides convective heat transfer from the wire and droplet surface, surface shear stress contributions and, perhaps, convective mass transfer to or from the surface. In order to predict these quantities involves the solution of equations (1) to (4) in the gas as well as in wire and droplet. This solution is eased if the gas flow problem can be considered to be quasi-steady relative to other aspects of the overall problem.

The typical values given above lead to gas bulk velocities of about 0.8 to 1.3 m/sec (2000 to 3000 in/min) which are an order-of-magnitude faster than the wire feed speed. This velocity leads to residence times of approximately 20 ms in passing along the solid wire and 2 ms in flowing past the droplet.

For globular metal transfer this residence time past the droplet is much less than the droplet period (\sim 100 ms) so, if needed, solutions for the convective heat and mass transfer in the gas could be accomplished with quasi-steady idealizations for forced convection. For spray transfer the

droplet periods of about 3 ms are comparable to the residence time so fully time-dependent treatments would be necessary. A further consequence of these observations is that, while empirical correlations from steady state experiments could be used for globular transfer, their application for spray transfer could be questionable and inaccurate.

2.6 Time scales - droplet

The time for a thermal change to approach steady state (within about five per cent) by conduction in the radial direction, the thermal conductive time scale, can be estimated as [Kreith, 1973]

$$\theta_T \approx 0.6 r_o^2 / \alpha$$

For an 1.6 mm (1/16 in.) diameter droplet of steel, this value would be about 50 ms which is of the same order-of-magnitude as the droplet period for globular transfer and is slower than the period for spray transfer.

The viscous time scale to approach steady state can be expected to be analogous to the thermal conductive time scale above, or

$$\theta_V \approx 0.6 r_o^2 / \nu = 0.6 \theta_T / Pr$$

where Pr is the Prandtl number for the liquid metal. (Allum [1985 a] quotes Sozou and Pickering [1975] as saying that for J x B flows to approach steady state requires $\theta \sim L^2 / \nu$, i.e., another viscous time scale.) For the same conditions as above, one obtains $\theta_V \approx 0.6 \text{ sec} \approx 600 \text{ ms}$, which is slow compared to the droplet periods.

These time scale estimates must be tempered with the recognition of the dependence of droplet sizes for the different modes of transfer and the r_o^2 dependence. Lesnewich [1958b] noted that globular transfer at low currents may yield droplets twice the diameter of the original wire so the viscous and conductive time scales would increase by a factor of four, to 2-1/2 sec and 200 ms, respectively. On the other hand, for spray transfer droplets may be as small as $d/4$, reducing these time scales by a factor of sixteen. Therefore, for spray transfer viscous time scales would be of the order $\theta_V \approx 40 \text{ ms}$ and the thermal conductive time scale would be about $\theta_T \approx 3 \text{ ms}$, comparable to the droplet period. However, it must be recognized that these time scales correspond to an approach to steady state through the entire cross section rather than near surface effects.

2.6.1 Resistive heating From an energy balance, one can show the time to raise a wire element to the melting temperature by resistive heating alone can be approximated as

$$\Delta\theta \approx \frac{\rho c A^2}{\rho_e i^2} (T_m - T_i)$$

if heat losses are neglected, properties are taken as constant, and the wire speed is considerably slower than the drift velocity of electrons. The distance required, or stickout, would be

$$L = V_w \cdot \Delta\theta = \frac{\rho c V A^2}{\rho_e i^2} (T_m - T_i)$$

If energy transfer from the arc is considered, the time and distance will be less yet.

For melting from solid to liquid, the time becomes

$$\Delta\theta \approx \frac{\rho A^2 \Delta u_{sl}}{\rho_e i^2}$$

where Δu_{sl} is the heat of fusion of the material. Heating to the boiling temperature and evaporation would be calculated in comparable fashion with Δu_{sl} replaced by Δu_{lv} , the heat of vaporization.

2.6.2 Wire motion The time for the wire to move a distance of one diameter is simply

$$\Delta\theta_{vel} = d/V_w$$

This time scale is on the order of milliseconds since the droplet diameter is of the order of the wire diameter and the droplet period is of the order of milliseconds (3-70 ms in the oft quoted experiment by Lesnewich [1958b], Figure 4).

2.6.3 Axial thermal conduction The propagation of a thermal pulse along the wire in the axial direction may be estimated with the classic solution for a step change in the surface temperature of a semi-infinite medium [Kreith, 1973]. A ninety percent response

$$\frac{T - T_s}{T_i - T_s} = 0.9$$

occurs at

$$\frac{x}{2\sqrt{\alpha\theta}} \approx 1$$

as

If one takes this value as an estimate of the response times, one finds the characteristic time given by

$$\Delta\theta_k \sim (\Delta x)^2 / 4\alpha$$

If one then compares this time scale to the motion, say again for a distance of a diameter, one finds

$$\frac{\Delta\theta_k}{\Delta\theta_{vel}} = \frac{V_w d_w^2}{4L\alpha} \rightarrow \frac{V_w d_w}{4\alpha} = \frac{Pe}{4} = \frac{RePr}{4}$$

or the thermal response is much faster than the wire motion if the Peclet number is much less than 4. This situation could lead to domination of conduction in the thermal problem for the wire. On the other hand, in the comparable convective heat transfer problem, axial conduction can usually be neglected when $Pe > 200$ [Kays, 1966].

2.6.4 Radial thermal conduction near surface Temperature variation near the surface affects the surface tension and, therefore, the droplet shape - particularly near the neck at detachment. Consequently, one must consider times to modify the surface layers rather than only the approach to steady state. For radial conduction in a cylinder, a 90% change in temperature is predicted at $r/r_0 = 0.9$ within non-dimensional time

$$\frac{\alpha\theta}{r_0^2} \approx 0.1 \rightarrow 0.15$$

This time scale is about 1/6 of that for full thermal penetration.

For the conditions in the experiments by Lesnewich [1958b], we can estimate

	Period	$\Delta\theta=0.6r_0^2/\alpha$	$\Delta\theta=0.1r_0^2/\alpha$	Thermal penetration
$d_w = 1.6\text{mm}(1/16\text{in})$	---	50ms	8ms	---
$2-1/2d_w = \text{globular}$	70ms	300	50	Partial
$2d_w/3 = \text{spray}$	3	20	3	Partial

These estimates indicate a need to include solution of the thermal energy equation as part of the transient numerical approach.

2.6.5 Electrical conduction For their weld pool simulation Kou and Wang [1986] claim the characteristic times associated with electrical conduction are of the order of 10^{-12} sec. Since these time scales probably have an r^2 dependence and the weld pool covers a larger region than the droplet, the corresponding times can be expected to be less than 10^{-12} sec in the present problem. Therefore, prediction of the current density field can be expected to be quasi-steady relative to the droplet period.

2.6.6 Current variation Typical power supplies show a "ripple" of about five percent in the electric current (unless they are stabilized) at 60 or 120 Hz. This situation implies about a 10% variation in i^2 with a period of 16 or 8 ms, respectively. Thus, this process is slow relative to spray detachment and slow relative to globular detachment, but in either case it could be expected to affect a periodic detachment process upon which it is superposed.

2.6.7 Pulsed supplies Ueguri, et al. [1985] used pulsed current supplies over the range 30 to 500 Hz, giving periods of 30 to 2 ms, respectively. At the higher frequencies, these are comparable to the period for spray transfer.

2.6.8 Surface tension The natural frequency of the fundamental mode for surface oscillation of a sphere of liquid surrounded by an infinite region of gas can be approximated as [Lamb, 1932, Sec. 275; Clift, Grace and Weber, 1978]

$$f^2 = \frac{16\sigma}{\pi^2 \rho d^3}$$

A time scale to correspond to a significant surface oscillation may be taken as 30/360 of the period of oscillation.

For a 16 mm (1/16 in.) diameter sphere of liquid steel, this relation gives a period of 4 ms and initial response time of about 0.4 ms. Since f varies as $d^{-3/2}$ these values convert to

	<u>Period</u>	<u>Initial response</u>
Globular	16 ms	2 ms
Spray	2 ms	0.2 ms

In both cases characteristic times are comparable to the time scale of the droplet growth. Globular drops would go through several surface oscillations and spray mode droplets would undergo about one cycle. (The question becomes: what is the amplitude of the oscillation?)

2.6.9 Thermocapillary ("Marangoni") flow Pimputkar and Ostrach [1980] analyzed transient thermocapillary flow ("Marangoni convection") in thin liquid layers. They found the appropriate time scale for small times to be $\Theta_M = h^2/\nu$ (where h is the height of the layer), i.e., another viscous time scale. The thermal time scale was $\Theta_{MT} = h^2 Pr/\nu$. The large

time solution has a scale $\Theta_{ML} = L/U$ where L is a measure of the stream-wise length and the characteristic velocity of the thermocapillary driving force is

$$U = \left| \frac{\partial \sigma}{\partial T} \right| A (T_H - T_C) / \mu$$

For this problem there was a significant velocity change in terms of

$$\frac{\partial \theta}{\partial x} = \frac{u}{U} \cdot \frac{\partial}{\partial \tilde{x}} \left[\frac{T - T_C}{T_H - T_C} \right]^{-1}$$

before $\theta \approx 0.1\theta_M$ and a steady Couette flow was approximately reached by $\theta \approx \theta_M$; significant surface distortion was predicted for $\theta > 0.01 L/U$ or less. The time $\theta \approx 0.1\theta_M$ would be about 60 ms for globular transfer and for spray transfer it would be about 4 ms, so Marangoni convection may be significant.

Again the velocity scale of Lai, Ostrach and Kamotani [1985] is

$$\bar{U} = \left| \frac{\partial \sigma}{\partial T} \right| \frac{A(T_h - T_c)}{\mu}$$

With an aspect ratio of unity and $T_h - T_c \approx 800C$ (1400 F) it gives a reference velocity of about 35 m/sec (115ft/sec $\approx 8 \times 10^4$ in/min). This is the surface velocity for steady state as implied by their "small time" solution. If one interpolates the results presented by Pimputkar and Ostrach [1980], one can predict the time necessary for the surface velocity to be comparable to the wire velocity. For $V_w = 0.008$ m/sec (200 in/min) it is approximately $0.001\theta_v$, where θ_v is the viscous time scale. This time interval is approximately 4 ms for globular sizes and 0.3 ms for spray droplets, with the velocity continuing to increase linearly at low values of θ/θ_v . The fallacy in this reasoning is probably that the analysis is based on instantaneous imposition of the surface temperature distribution, which is not realistic for the droplet transfer problem.

A more appropriate approach may be to reinterpret the characteristic velocity in terms of the axial temperature gradient and then to estimate the related residence time for a fluid particle to traverse half the circumference. The grouping

$$\left| \frac{\partial \sigma}{\partial T} \right| \frac{T_h - T_c}{\mu}$$

can be considered to be an approximation of $\partial\sigma/\partial x$. Since

$$\frac{\partial\sigma}{\partial x} \approx \frac{\partial\sigma}{\partial T} \cdot \frac{\partial T}{\partial x}$$

an alternate estimate of the velocity scale would be $\bar{U} = |\partial\sigma/\partial x|d/(2\mu)$ or

$$U = \left| \frac{\partial\sigma}{\partial x} \right| \frac{d}{2\mu} \approx \frac{8}{\pi^2} \left| \frac{\partial\sigma}{\partial T} \right| \frac{i^2 \rho_e}{\rho_w c_p \mu V_w d^3}$$

near the solid wire (i.e., $A_{CS} \approx A_w$). With this velocity the surface tension Reynolds number may be defined

$$Re_\sigma = \frac{\bar{U}L}{\nu} = \frac{\pi \bar{U}d}{2\nu} \approx \frac{4}{\pi} \left| \frac{\partial\sigma}{\partial T} \right| \frac{i^2 \rho_e}{c_p \mu^2 V_w d^2} \frac{\rho_l}{\rho_w}$$

Following the same reasoning, one may define residence time for half the circumference to be

$$\Delta\theta \approx \frac{\pi d}{2U} \approx \frac{\pi^2}{16} \frac{\rho_l c_p \mu V_w d^4}{|\partial\sigma/\partial T| i^2 \rho_e}$$

These revised quantities were evaluated for a current of 250 amps, wire speed of 0.08 m/sec and the 1.6 mm steel wire. The reference velocity \bar{U} became 1.8 m/sec (5.8 ft/sec \approx 4200 in/min) which gave $Re_\sigma \approx 7000$. The residence time scale for a 1.6 mm diameter became 1.4 ms. If one holds d_w and V_w (and therefore \dot{m}) constant, U varies approximately as $1/d$ for droplets of various diameters and $\Delta\theta$ varies as d^2 . For globular droplets one may estimate $\Delta\theta \approx 2$ ms and for spray $\Delta\theta \approx 0.4$ ms. However, these estimates correspond to a steady thermocapillary flow which may approximately occur near the solid wire, but it is presumeably disrupted by the detachment for the droplet region.

Another approach which may indicate an upper band is to take the revised velocity scale with the analysis of Lai, Ostrach and Kamotani [1985, Fig. 4] and to estimate the predicted residence time corresponding to the flow induced during a typical droplet period. The initial condition is a fluid at rest. For globular transfer this approach gives $\Delta\theta \approx 60$ ms or the same order as the period. For spray, we estimate $\Delta\theta \approx 20$ ms which is significantly longer than the period. These values imply that thermocapillary convection could be important for globular detachment but is not likely to be for spray transfer.

The direction of flow due to thermocapillary convection depends on whether the surface tension increases or decreases with temperature. In a sense, a region with higher σ pulls fluid from regions with lower σ . For typical steels $\partial\sigma/\partial T$ is negative so the flow tendency would be from warmer to cooler. In the

vertical geometry considered here, that would be from the warm liquid drop towards melting zone and might inhibit detachment. With small amounts of contaminants, as in the weld pool studies of Heiple and Roper [1982], $\partial\sigma/\partial T$ can become positive so the tendency would be towards enhancing detachment forces.

3. NUMERICAL TECHNIQUE

3.1 Background

A tentative approach to solution of the thermofluidmechanics aspects of the problem is presented in the earlier section 1.6.4, on Task d. This approach is not chiseled in stone, rather it is illustrative. The actual form of the governing equations to be solved is currently evolving in Task (c) from the results of tasks (a) and (b). The actual method of solution will depend on the final form of the governing equations. The boundary conditions to be applied have been described earlier.

The study of time scales discussed previously may now be employed in order to simplify the governing equations. Firstly, the magnitude of the Reynolds number and the length of the viscous diffusion time scale compared to the estimated droplet detachment period suggest that viscous phenomena will have a negligible effect on the fluid momentum. Thus, it would appear that the term $\mu \nabla^2 u$ in the momentum equation may be dropped. (However, it is retained as described later.) Similarly, the smallness of the Prandtl number for liquid metals allows the dissipation term, Φ , to be neglected in the thermal energy equation [Kays and Crawford, 1980].

In Maxwell's equations (5) through (9) we assume that the droplet is electrically neutral so that $\rho_e = 0$. We may also make the assumption that all velocities, characteristic of the weld drop detachment, are much slower than the speed of light. This assumption allows us to drop the term $\partial(\epsilon E)/\partial t$.

With these assumptions and approximations the governing equations would become

Momentum

$$\rho \frac{D\vec{u}}{Dt} = -\nabla p + \rho \vec{g} + \mu_m \vec{J} \times \vec{H}$$

Continuity

$$\nabla \cdot \vec{u} = 0$$

Thermal energy

$$\rho C_V \frac{DT}{Dt} = \nabla \cdot (k \nabla T) + \frac{J^2}{\sigma}$$

Species

$$\frac{DC}{Dt} = \kappa_S \nabla^2 C$$

Electromagnetic

$$\nabla \times \vec{E} + \frac{\partial(\mu_m \vec{H})}{\partial t} = 0$$

$$\nabla \times \vec{H} = \vec{J}$$

$$\nabla \cdot (\mu_m \vec{H}) = 0$$

$$\nabla \cdot (c \vec{E}) = 0$$

$$\vec{J} = \sigma_e (\vec{E} + \mu_m \vec{u} \times \vec{H})$$

It is believed that the above equations, when solved in conjunction with the appropriate boundary conditions, contain the essential physics necessary to model droplet detachment phenomena accurately for many cases. The boundary conditions appropriate for the above set of equations are largely the same as those appropriate for the full set. The major exception to this statement arises with regard to the momentum equation.

If we neglect viscous effects and therefore exclude the viscous shear term, we must also exclude a boundary condition. This requirement results from the reduction of the momentum equation from second to first order by the exclusion of the viscous term. The appropriate boundary condition to exclude is that concerning the tangential stresses at the free surface of the weld drop. This situation is analogous to that which occurs in the reduction of the Navier-Stokes equations to potential flow. However, to account for Marangoni convection we anticipate retaining the viscous terms and associated boundary conditions.

The remaining fluid boundary condition determines the pressure or normal stress at the droplet surface. It can be written as

$$P = P_g + \sigma K$$

where P_g is local pressure in the shielding gas, σ is the surface tension and K is the local mean curvature of the droplet surface.

It is anticipated that these equations will be solved through the use of a finite-volume technique which is currently under development. Such techniques allow one to handle complicated geometries without requiring that the governing equations be written in curvilinear coordinates. Domain fitted meshes will be employed in order to simplify the application of boundary conditions. Such meshes may be obtained through the use of potential flow mappings. Potential mappings may be obtained economically through the use of numerical boundary integral methods. An example of such a method being employed to examine the comparable problem of the unsteady growth of an axisymmetric bubble from an orifice may be found in Figure 6, calculated earlier by Uhlman [Meng and Uhlman, 1986].

In addition, adaptive regridding procedures may be employed in order to resolve adequately regions which develop high gradients during the course of the calculation.

Initial numerical analyses will concentrate on developing the thermal-fluidmechanic solution and simple approximations will be made to include effects of the electromagnetic fields. It is anticipated that diffusive time scales for electrical and magnetic effects will be much faster than viscous and thermal time scales so that the electromagnetic treatment can be considered quasi-steady relative to the thermofluids problem. As a first approximation, it is expected that constant current density at a cross section will be a reasonable assumption for much of the geometry. For static magnetic field problems (i.e., quasi-steady), Maxwell's formulae can be reduced to Poisson's equation, an elliptic partial differential equation. For the present approach, at each time step the momentum and energy equations to be solved will be elliptic in character. Thus, the numerical structure to be used for the thermofluids solution should be applicable to the electromagnetic problem as well; if not, a number of programs such as MARE-C, MAGNET, POISSON, PE2D, FLUX. etc., are available to provide guidance in developing our own.

The first version of the code being developed will treat conditions comparable to globular transfer with gravity and surface tension forces dominating. This problem requires the same general treatment of the energy and momentum equations as the more complete solution. For example, body force terms must be included in the momentum equation for gravitational forces; these same body force terms can then be extended to account for electromagnetic forces provided from solution of Maxwell's equations. With a solution procedure for the globular problem, the numerical code can be tested by adjusting parameters to correspond to conditions of simple analyses as by Greene [1960] and of related model experiments [Harkins and Brown, 1919; Calverley, 1957].

3.2 General approach

The problem to be solved covers the transient growth of the liquid droplet. From the study of Allum [1985] it is anticipated that it will grow "slowly" until a critical condition is reached, probably at its minimum diameter. Then an instability will lead to detachment within a very short time scale. Initial calculations aim at describing the droplet behavior until the criticality condition is reached. If the instability is very

rapid compared to the droplet growth, it will be the earlier growth which dominates the droplet period and its properties. Then shifting to a shorter time interval, to follow the instability, may allow testing the various hypotheses offered concerning this instability.

The moving solid wire and attached liquid droplet are being described by a numerical representation using finite control volumes and finite time intervals to approximate the non-steady governing equations. Axi-symmetric orthogonal coordinates are employed, but a non-orthogonal mesh scheme is used in order to follow the development of the droplet and its free surface.

The general computer code is being developed in stages so its components can be verified by comparison to classical analyses and experiments. The following solution steps are envisioned:

- 1) Momentum and continuity equations for liquid droplet flow from a tube. Adds the complications of variable non-orthogonal grid, transient flow and free surface.
- 2) Thermal energy equation with resistive heat sources and boundary heating. Adds solid-to-liquid phase change and Marangoni convection.
- 3) Maxwell's equations. Adds electromagnetic forces and electrical current distribution.
- 4) Species transport equation. Accounts for surface additives on wire electrode.

To allow for Marangoni convection, the viscous terms are retained in the momentum equations. This action also simplifies the code development because the momentum equations then have the same character as the energy equation and the same solution routines can be employed.

In axi-symmetric coordinates the Eulerian forms of the thermofluid equations become

Continuity,

$$\frac{\partial u}{\partial x} + \frac{1}{r} \frac{\partial (rv)}{\partial r} = 0 \quad \text{or} \quad \frac{\partial (ru)}{\partial x} + \frac{\partial (rv)}{\partial r} = 0$$

Axial momentum,

$$\begin{aligned} \frac{\partial}{\partial t} (\rho u) + \frac{\partial}{\partial x} (r\rho u^2) + \frac{\partial}{\partial r} (r\rho uv) &= -r \frac{\partial p}{\partial x} + r\rho g \\ + \frac{\partial}{\partial x} (r\mu \frac{\partial u}{\partial x}) + \frac{\partial}{\partial r} (r\mu \frac{\partial u}{\partial r}) &+ J_r B_\theta \end{aligned}$$

Radial momentum,

$$\begin{aligned} \frac{\partial}{\partial t}(\rho r v) + \frac{\partial}{\partial x}(r \rho u v) + \frac{\partial}{\partial r}(r \rho v^2) &= -r \frac{\partial \rho}{\partial r} \\ + \frac{\partial}{\partial x}(r \mu \frac{\partial v}{\partial x}) + \frac{\partial}{\partial r}(r \mu \frac{\partial v}{\partial r}) - \frac{\mu v}{r} - J_x B_\theta \end{aligned}$$

Thermal energy

$$\begin{aligned} \frac{\partial}{\partial t}(\rho r i) + \frac{\partial}{\partial x}(r \rho u h) + \frac{\partial}{\partial r}(r \rho v h) \\ = \frac{\partial}{\partial x}(r \frac{k}{c_p} \frac{\partial h}{\partial x}) + \frac{\partial}{\partial r}(r \frac{k}{c_p} \frac{\partial h}{\partial r}) + \Phi + \frac{|J|^2}{\sigma} \end{aligned}$$

To account for the time-dependent volume of the droplet, the grid will be re-adjusted at each new time step. While a finite-control-volume representation is employed at each instant, the control volumes deform in order to match the free surface development and move with the flow (approximately). Therefore, the control volumes are neither fixed in space nor do they correspond to control masses; that is, the grid treatment is neither Eulerian nor Lagrangian.

A simple grid scheme is used for the initial derivation of the algebraic equations. Each control volume is formed from four intersecting conical surfaces with their vertices on the axis of symmetry (at infinity for purely radial surfaces in the solid wire). In an axial plane the cross-sections are approximately rectangular, with the exception of corner regions. For deriving the algebraic equations, the circumferential distance is a unit angle for each control volume. Figure 7 demonstrates a possible grid in an early stage of the transient process.

A staggered grid [Patankar, 1980; Huang and Leschziner, 1982] is employed with nodes for the velocity components displaced from the scalar nodes. Figure 8 demonstrates the pattern. The control volumes for the scalars, such as p , T and C , are laid out first as shown by the solid lines. Their nodes are then placed at their centroids. Nodes for the velocity components are placed at the centers of the scalar control surfaces; thus, a typical control volume for the axial momentum equation is formed as shown by the dashed lines.

In axi-symmetric coordinates the general representation of the governing equations, as in section 3.1, is

$$\frac{\partial}{\partial t}(r\rho\phi) + \frac{\partial}{\partial x}(r\rho u\phi) + \frac{\partial}{\partial r}(r\rho v\phi) \\ = \frac{\partial}{\partial x}\left(r\Gamma\frac{\partial\phi}{\partial x}\right) + \frac{\partial}{\partial r}\left(r\Gamma\frac{\partial\phi}{\partial r}\right) + rS$$

where ϕ stands for the dependent variable, u , v , T , c , etc., and S is a source term which includes the terms which do not fit the pattern above. Therefore, the same solution algorithm can be applied to solve each of the governing equations. The continuity equation is combined with the momentum equations to yield a "pressure-correction" equation which also takes the same form [Patankar, 1980].

If f is some differentiable scalar function, the control volume formulation of the governing equations can be developed via the transport theorem to account for the changing shapes and sizes of the control volumes. We define

$$I(\vec{x}, t) = \iiint_{V(t)} f(\vec{x}, t) dV$$

The transport theorem then states that

$$\frac{dI}{dt} = \iiint_{V(t)} \frac{\partial f}{\partial t} dV + \iint_{S(t)} f U_n dS$$

where S is the boundary surface of V and U_n is the normal velocity of the surface [Newman, 1978, pp. 56-60].

The conservation laws may be expressed as

Rate of change of f in V	=	Rate of influx of f through S into V	+	Rate of production of f from sources in V
--------------------------------	---	--	---	---

or

$$\frac{d}{dt} \iiint_V f dV = \iint_S \Sigma_f dS + \iiint_V \sigma_f dV$$

Next we define a vector field, $\vec{\beta}$, by

$$\Sigma_f = \vec{n} \cdot \vec{\beta}$$

where \vec{n} is the unit normal to S. If $f(\vec{x}, t)$ is a quantity which can be advected, the flux Σ_f may be decomposed as

$$\Sigma_f = -\vec{n} \cdot \vec{w} f + \Sigma'_f$$

where \vec{w} is the relative velocity between the fluid and the surface S of the control volume such that

$$\vec{n} \cdot \vec{w} = \vec{n} \cdot \vec{u} - U_n$$

where \vec{u} is the velocity of the fluid.

The conservation equation may then be written

$$\begin{aligned} \iiint_V \frac{\partial f}{\partial t} dV + \iint_S U_n dS &= \\ \iint_S \left\{ -\vec{n} \cdot (f \vec{u}) + f U_n + \Sigma'_f \right\} dS & \\ + \iiint_V \sigma_f dV & \end{aligned}$$

In order to derive the algebraic approximation of each governing equation, these integrals are evaluated by volume and area averages as appropriate. Inflow terms involving gradients, such as diffusion, are approximated by simple finite differences (or appropriate averages thereof to account for the non-orthogonal nature of the grid).

The algebraic governing equations are solved by marching forward in time from initial conditions (or initial estimates). Implicit representations [Richtmyer, 1957] are employed to reduce the complexity of the equations and to enhance numerical stability of the solution algorithm. Therefore, at each time step only information from the prior time step and the present are

required to calculate the terms in the equations. To account for the non-linear nature of the convective terms, for the temperature dependence of some of the properties and for the motion of the free surface, provision for iteration is included in the code.

For internal control volumes, the algebraic equation for each control volume at each time step involves nine nodes as shown for the scalar control volume in Figure 8. This 3 x 3 pattern of unknowns permits application of a tridiagonal matrix algorithm [Richtmyer, 1957], swept successively in alternate directions, to form the solution for the desired field. The technique is comparable to that used by Huang and Leschziner [1982] in the TEAM code and other elliptic equation solvers, and is sometimes referred to as a line-by-line TDMA method.

3.3 Status

Development of the computer code for step 1, momentum and continuity equations, is in process. The computer language is Fortran and the DEC VAX-11/8600 at our Cleveland Operation is used for program development.

The subroutine organizing the numerical mesh has been derived in terms of transient axi-symmetric coordinates, r , x and t , with indices i , j and k . Typically, this leads to arrays of size $M \times N \times 2$ for each variable. Subroutines for calculating needed surface areas, volumes and centroids are complete. The convection and diffusion terms in the algebraic equation for general scalar variables have been derived but are not yet coded. For the momentum equations, the convection terms have been derived and coded while derivation of the diffusion terms and diffusion source terms is nearly complete. The line-by-line, TDMA solution algorithm has been programmed.

The next steps are treatment of the boundary control volumes and development of the algebraic version of the pressure-correction equation which represents the continuity equation. Computer output routines will be specialized from various generic versions held in-house.

4. CONCLUDING REMARKS AND RECOMMENDED PLANS

A combined analytical and numerical study of droplet detachment in gas metal arc welding was initiated. Globular and spray modes were considered, concentrating on 1.6 mm (1/16 in) diameter steel wires as in the classic experimental papers of Lesnewich [1958]. Previous investigations have shown that gravitational forces and surface tension forces dominate in the globular mode with electromagnetic forces also becoming important for spray transfer.

Approximate analyses and time scale estimates were conducted to guide the development of a general numerical technique for examining the problem and for obtaining predictions for appropriate ranges of parameters. Viscous and thermal time scales were found to be longer than the droplet periods, but solution of the (viscous) momentum equations and thermal energy equation will be necessary for treatment of surface phenomena.

Approximate values of non-dimensional parameters showed surface tension to be important - as was known. Time scales analyses indicated that convection

induced by thermocapillary action ("Marangoni convection") may be significant, but that natural convection within the drop was not likely to be. Surface oscillations and power supply frequencies were seen to be comparable to the frequencies of droplet detachment; if their related amplitudes are large enough, these phenomena could contribute to scatter in droplet volumes and periods measured in experiments. Convective heat transfer to the shielding gas was found to be a quasi-steady situation for globular transfer but non-steady for the spray mode. To date the time scales analyses and approximate analyses have not revealed any significant simplifications to the partial differential thermofluid equations describing the general problem.

Development of a numerical code was started to treat the general problem of axisymmetric droplet detachment. The approach is comparable to the versatile TEAM code of UMIST with the additional complexities of free surfaces and continuously varying grids, phase change and transient phenomena. The derivation is proceeding using the TEAM and VADUCT-E codes for guidance.

The first step is to solve the axisymmetric momentum and continuity equations for transient liquid flow issuing from a tube. This version introduces the features of free surfaces and time-varying grids with gravitational and surface tension forces corresponding to globular transfer. Geometric variables and parameters have been coded and the line-by-line, TDMA solution algorithm has been programmed. Convection terms for the momentum equations have been derived and coded; derivation of diffusion terms and diffusion source terms is in process.

The next steps in our plan are to complete the development of the momentum equations representation, to treat the boundary control volumes and to derive the algebraic version of the pressure-correction equation which represents the continuity equation. The program performance will then be tested by comparison to results for classical cases to which it can be specialized. This version will also simulate experiments for the determination of isothermal liquid surface tension and should provide means to evaluate assumptions typically employed in data reduction for such experiments.

TABLE 1.

Approximate Thermofluid Properties of Mild Steel [Waszink and Piena, 1985]
and/or Iron

Solid

T_1	=	1536 C = 2797F
H_{mp}	=	1.3×10^6 J/kg
α_{wire}	=	7.3×10^{-6} m ² /sec
ρ_{wire}	=	7870 kg/m ³
k_{wire}	=	40 W/(mC)
$c_{p_{wire}}$	=	700 J/(kg C)

Liquid Iron

ρ	=	6500 kg/m ³ 7450 dynes/cm ³ Steel, "weight density" [Greene 1960]
c_p	=	800 J/(kg C)
k	=	40 W/(m C)
α_{exp}	=	1.3×10^{-4} C ⁻¹
ν	=	0.6×10^{-6} m ² /s
α	=	8×10^{-6} m ² /s
Pr	=	0.075
ρ_R	=	1.4×10^{-6} $\Omega.m$
Surface tension		at 1650C (3000F)
σ	=	1.9 N/m pure iron 1.3 N/m 0.1% O ₂ 1.2 N/m Steel [Greene, 1960]

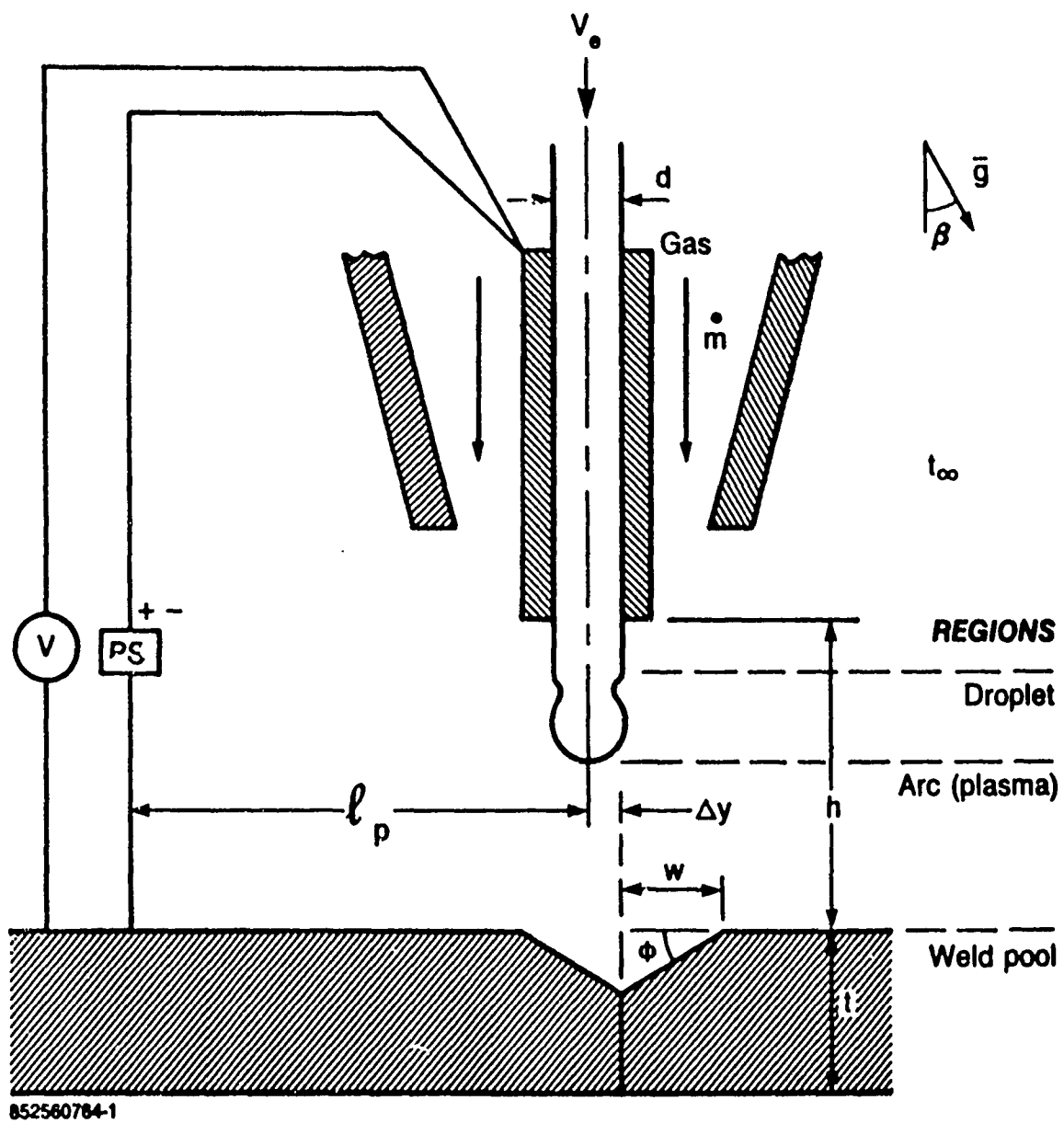
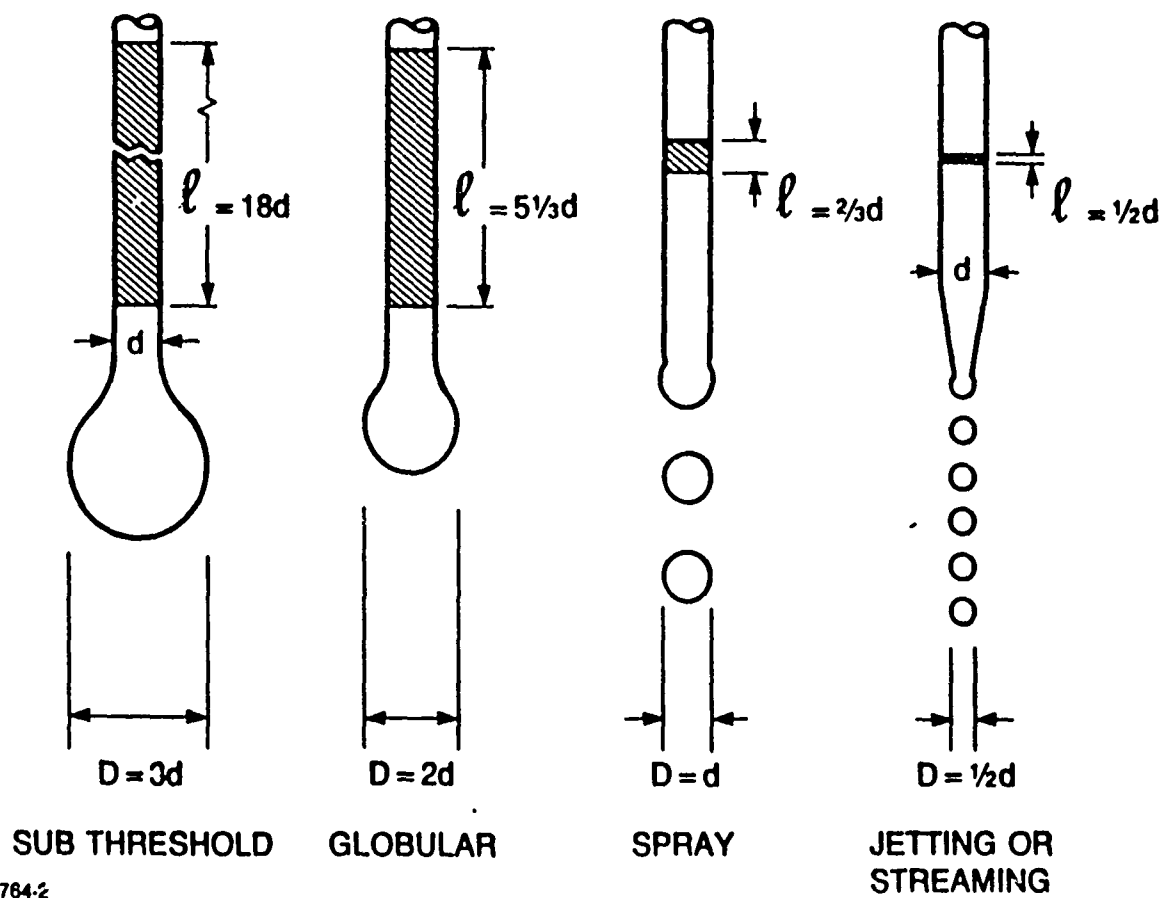


FIGURE 1 Schematic description of control parameters in gas metal arc (GMA) welding



852580764-2

Figure 2. Range of metal transfer according to length of wire per drop [Needham and Carter, 1965]

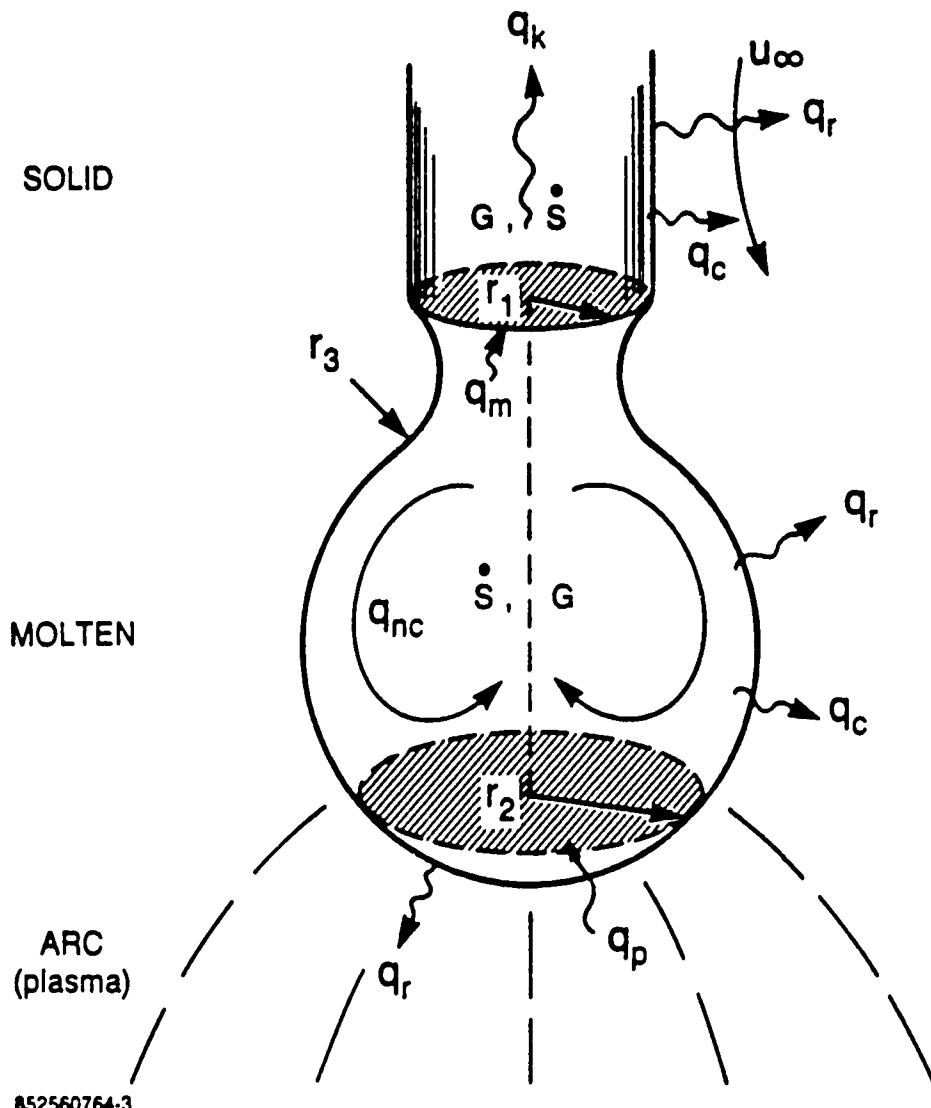


Figure 3. Thermal processes in an idealized, vertical droplet

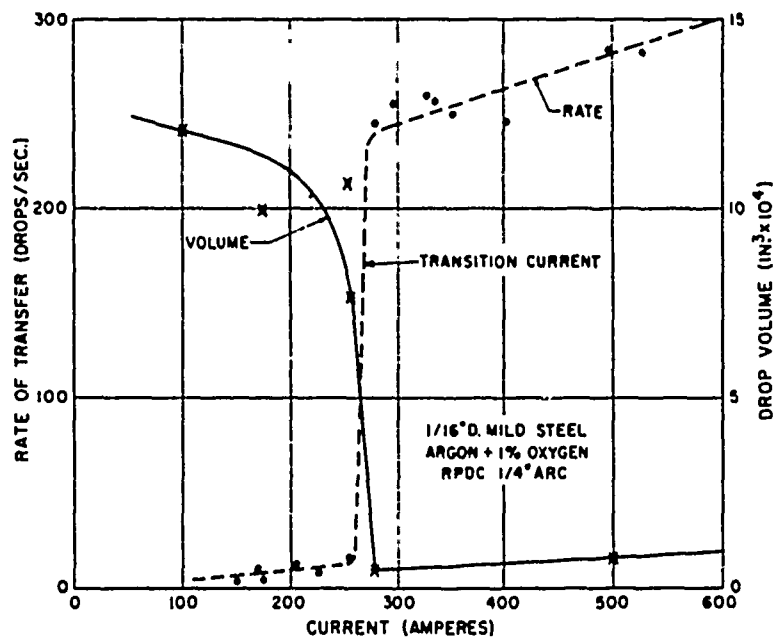
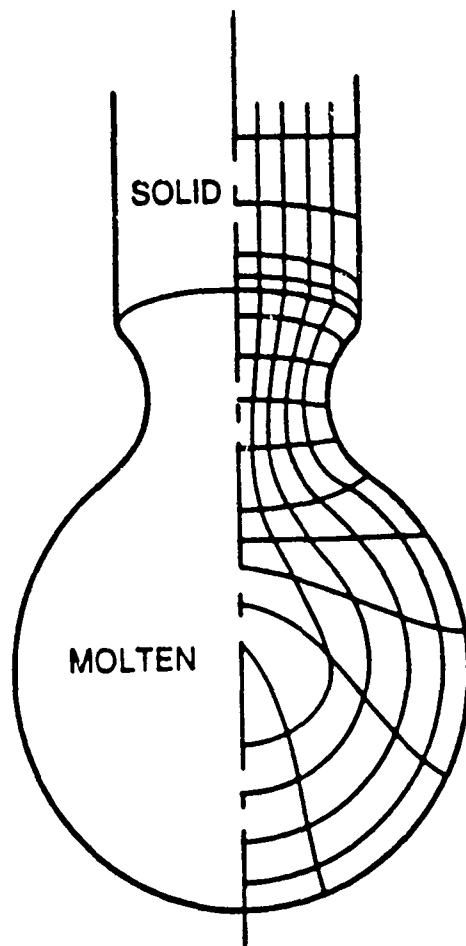


Figure 4. Effect of current on the size and frequency of drops transferred from a 1-1/2 mm (1/16 inch) steel electrode in an argon shielded arc [Lesnewich, 1958b]



852560764-4

Figure 5. Illustrative example of adaptive, curvilinear finite-control-volume grid for detachment process of metal transfer in gas metal arc welding

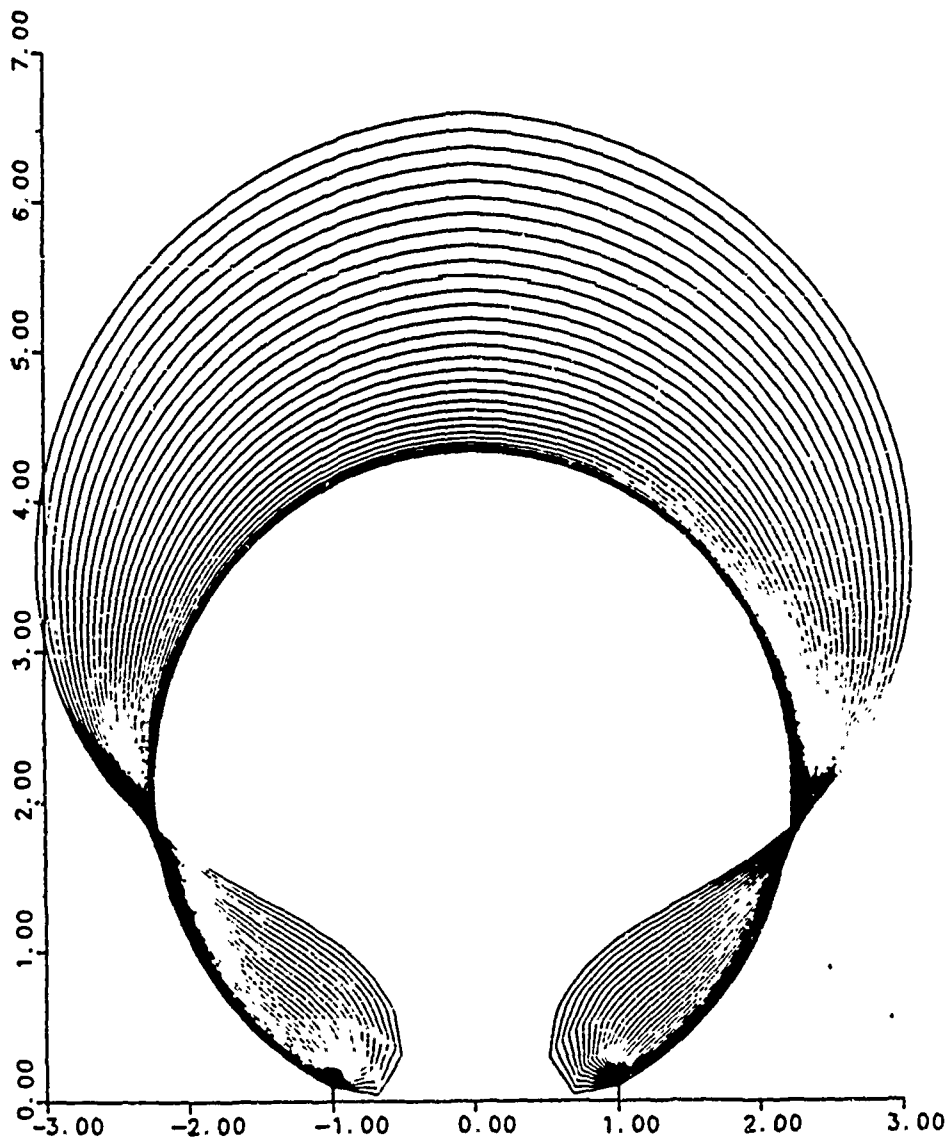


Figure 6 Numerical prediction of bubble growth at a wall under the influence of gravity and surface tension [Meng and Uhlman, 1986]

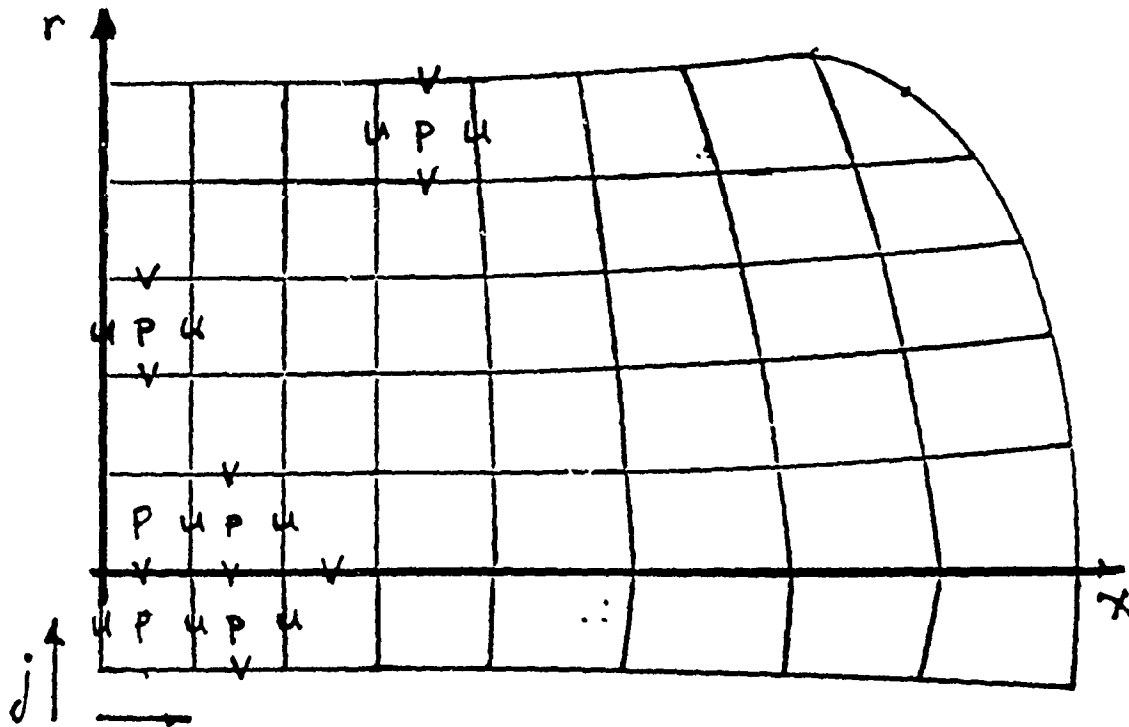


Figure 7. Typical grid scheme in early stage of development

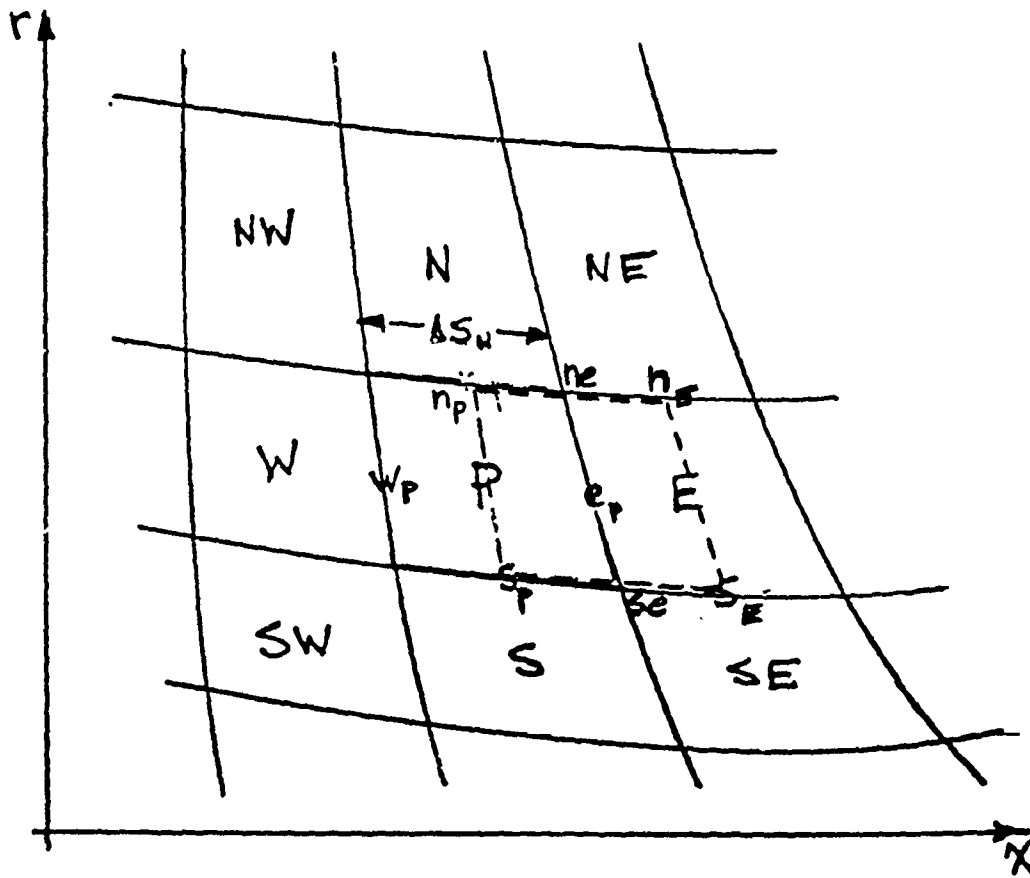


Figure 8. Mesh and control volumes in staggered grid

REFERENCES CITED

- Allum, C.J., 1985a. J. Phys. D: Appl. Phys., 18 pp 1431-1446.
- Allum, C.J., 1985b. J. Phys. D: Appl. Phys., 18 pp 1447-1468.
- Brown, R.A., 1972. J. Atmos. Sci., 29, pp. 850-859.
- Calverley, A., 1957. Proc., Phys. Soc. B, 70, pp 1040-1044.
- Cameron, J.M. and A.J. Baeslack, 1956. Welding J. pp 445-449.
- Clift, R., J.R. Grace and M.E. Weber, 1978. Bubbles, drops and particles. New York: Academic.
- Cooksey, C.J., and Miller, D.R., 1962. Metal Transfer in Gas-Shielded Arc Welding, Physics of the Welding Arc--A Symposium 1962, pp. 123-132.
- Eagar, T.W., 1985. Personal Communication, Mass. Inst. Tech., August 1985.
- Eagar, T.W., 1987. Personal Communication, MIT, 5 Nov.
- Greene, W.J. 1960. Trans. AIEE, 79, pp 194-203.
- Halmoy, E., 1980. Wire melting rate, droplet temperature and effective anode melting potential. Arc Physics and Weld Pool Behavior, Cambridge: Welding Inst., pp. 49-57.
- Harkins, W.D., and F.E. Brown, 1919. J. Amer. Chem. Soc., 41, pp 499-524.
- Heiple, C.R. and J.R. Roper, 1982. Welding J., 61, pp. 97s-102s.
- Huang, P.G., B.E. Launder and M.A. Leschziner, 1985. Comp. Meth. Appl. Mech. Eng., 48, pp. 1-24.
- Huang, P.G., and M.A. Leschziner, 1983. An introduction and guide to the computer code TEAM. Tech. rept., UMIST.
- Kays, W.M., 1966. Convective heat and mass transfer. New York: McGraw-Hill.
- Kays, W.M., and M.E. Crawford, 1980. Convective heat and mass transfer, 2nd. Ed. New York: McGraw-Hill
- Kline, S.J., W.C. Reynolds, F.A. Schraub and P.W. Runstadler, 1967. J. Fluid Mech., 30, pp. 733-741.
- Kohda, H., 1985. J. Crystal Growth, 71, pp. 813-816.
- Kovitya, P., and J.J. Lowke, 1985. J. Phys. D: Appl. Phys., 18, pp 53-70

- Kreith, F., 1973. Principles of Heat Transfer. Scranton: Intext.
- Kou, S., and Y.H. Wang, 1986. Welding J., 65, pp 63s-70s.
- Lai, C.L., S. Ostrach and Y. Kamotani, 1985. The role of free-surface deformation in unsteady thermocapillary flow. U.S.-Japan Heat Transfer Joint Seminar.
- Lamb, H., 1932. Hydrodynamics, 6th. ed. Cambridge Univ. Press.
- Lancaster, J.F., 1962. Influence of Heat Flow on Metal Transfer in Metal/Inert Gas Welding of Aluminum, Physics of the Welding Arc--A Symposium 1962, pp. 170-174.
- Lancaster, J.F., ed., 1984. The Physics of Welding. Oxford: Pergamon.
- Langlois, W.E., 1985. Ann. Rev. Fluid Mech., 17, pp. 191-215.
- Leonard, B.P., 1979. Comp. Mech. Appl. Mech. Engr., 19, pp. 59-98.
- Lesnewich, A., 1958a. Welding J., 37, pp 343s-353s.
- Lesnewich, A., 1958b. Welding J., 37, pp 418s-425s.
- Lesnewich, A., 1987. Welding J., 66, pp 386s-387s.
- Levich, V.R., and V.S. Krylov, 1969. Ann. Review Fluid Mech., 1, pp. 293-316.
- Masubuchi, K. and Terai, K., 1976. Future Trends of Materials and Welding Technology for Marine Structures, Philadelphia, PA, June 2-5, 1976, pp. 5-8 to 5-9.
- McEligot, D.M., 1985. Prediction of natural convection in diabatic inclined tubes. Tech. report, GOULD-OSD-771-HYDRO-CR-85-06.
- Meng, J.C.S., and J.S. Uhlman, 1986. Theoretical analysis and numerical simulation of bubble formation dynamics in a turbulent boundary layer. Tech. report, Gould-OSD-771-HYDRO-CR-86-04.
- Needham, J.C., 1962. Control of Transfer in Aluminum Consumable Electrode Welding, Physics of the Welding Arc--A Symposium 1962, pp. 114-122.
- Needham, J.C., and Carter, A.W., 1965. British Welding, pp. 229-241.
- Newman, J.N., 1978. Marine hydrodynamics. Cambridge: MIT Press, pp. 56-60.
- Oreper, G.M., T.W. Eagar and J. Szekely, 1983. Welding J., 62, pp 307s-312s.
- Oreper, G.M., and J. Szekely, 1984. J. Fluid Mech., 147, pp. 53-79.
- Ostrach, S., 1982. Heat Transfer 1982 (München), 1, pp. 365-379.

- Patankar, S.V., 1980. Numerical heat transfer and fluid flow. Washington: Hemisphere.
- Pfender, E., 1978. Gaseous Electronics (M.N. Hirsch and H.J. Oskam, ed.) Vol. 1, Ch. 5, New York: Academic Press.
- Pimputkar, S.M., and S. Ostrach, 1980. Phys. Fluids, 23, pp 1281-1285.
- Richtmyer, R.D., 1957. Difference Methods for Initial Value Problems. New York: Interscience.
- Ries, D.E., 1983. M.Sc. Thesis, Materials Engr., M.I.T.
- Sanders, N.A., and E. Pfender, 1984. J. Appl. Phys., 51 pp. 714-722
- Traugott, S.C., 1986. NASA CR Tech. Rpt.MFS-27095 (Contract NAS8-35773), Martin-Marietta Corp. NASA Tech. Briefs, 10 No. 3.
- Ueguri, S., K. Hara and H. Komura, 1985. Welding J., 64 pp. 242s-250s.
- van Doormaal, J.P. and G.D. Raithby, 1985. ASME paper 85-HT-9.
- Waszink, J.H., and G.J.P.M. van den Heuvel, 1982. Welding J., 61, pp 269s-282s.
- Waszink, J.H., and L.H.J. Graat, 1983. Welding J., 62, pp 108s-116s.
- Waszink, J.H., and M.J. Piena, 1985. Welding J., 64, pp. 97s-102s.
- Waszink, J.H., and M.J. Piena, 1986. Welding J., 65, pp 289s-298s.
- Woods, R.A., 1980. Welding J., 59, pp 59s-66s.